Constructing a conceptual food web of Oslofjord zooplankton using stable isotope analysis

Erik Engseth

Master Thesis
Marine biology and limnology
60 credits

Department of Biosciences
Faculty of Mathematics and Natural Sciences

UNIVERSITY OF OSLO

March 2024

Metridia longa

Constructing a conceptual food web of Oslofjord zooplankton using stable isotope analysis

Erik Engseth

http://www.duo.uio.no/

Trykk: Reprosentralen, Universitetet i Oslo

Abstract

It is commonly assumed that zooplankton is a homogeneous herbivore community at trophic level 2. I used stable isotope data to assess feeding ecology of the copepod community in the Oslofjord. I focused on 7 genera, of which 4 were sampled monthly from January to November 2022. I aimed to evaluate the trophic position of key copepod genera *Calanus, Acartia, Centropages, Temora, Oithona, Paraeuchaeta* as well as seasonal variation in trophic position within the copepod community. This is the first use of stable isotope data on a seasonal and genera-specific scale of the Oslofjord zooplankton community. I found two distinct trophic groups of copepods. The omnivorous group (i.e., *Temora, Centropages, Acartia, Calanus*) had a mean trophic level from 2 to 2.5, while the carnivorous group (i.e., *Chiridius, Metridia, Paraeuchaeta, Metridia*) had a mean trophic level of 3.1 to 3.5. There is also variation within genera based on species composition and seasonal variation. Biomass data of zooplankton at Släggö sampled by the Swedish zooplankton monitoring (SMHI) combined with my stable isotope data of the Oslofjord allowed me to assess the trophic level of the zooplankton community based on genus composition and trophic level of genera. I found a seasonal pattern with a lower trophic level in the summer than winter. The genus *Calanus* is the most omnivorous genus and stable isotopes suggest a carnivorous strategy in the winter, herbivorous feeding during the spring bloom and an omnivorous strategy in the summer. My data shows that the zooplankton feeding biology can be explained through genus-specific feeding and to some extent through shared traits such as feeding mode. The zooplankton community differs by 1 trophic level from winter to summer. Zooplankton can not be used as a baseline in food webs and trophic transfer studies without accounting for genus-composition and interactions with the microbial community.

Preface

While I prepared zooplankton samples, I got news that the isotope lab would be closed and unavailable after a month. Therefore the preparation of samples was rushed and compromised. The strategy that I used to acquire representable data consisted of sampling a wide selection of species while sampling a longer time interval of larger copepods. That is why the dataset has a higher coverage for larger genera. Zooplankton from a station called DK1 was also sampled during the cruise, but not prepared for stable isotope analysis due to time and possibly budget limitations. Thanks to help from staff Berit and Per as well as others, and especially the isotope lab engineer Bill Hagopian who put in overtime to finish the analysis of peoples samples, the resulting dataset was good for my purpose. Even then, I would have liked to obtain more data for smaller copepods, also at the DK1 station, especially for the year-round copepod *Oithona*.

I also prepared samples of healthy and parasitized Calanus for this thesis. However, I decided to focus my thesis on genera and their trophic position instead. These samples were part of a paper written by Eliassen et al. (2024) (Appendix A) and data of their $\delta^{15}N$ is also presented in Appendix B.

Acknowledgements

I would like to thank my very supportive supervisors Tom and Josefin, who have helped me through this thesis even though it took a longer than anticipated time to write it. Thank you Tom for helping me with all the R-coding and modeling and thank you Josefin for advice on writing and literature searching.

For help with lab work I would like to thank Berit Kaasa, Per Færøvig and Thi Thuy Minh Vu for help with equipment and work. I give special thanks to William Martin Hagopian for taking extra time to analyze all my samples despite the trouble with asbestos sanitation of the lab. I also would like to thank Tonje Storholt and Hanne Børseth for collecting and sharing stable isotope data of seston from Tonje's experiments with me. I thank the crew of Trygve Braarud, captain Sindre Holm and cruise leader Even Garvang and various people who have been involved in collecting zooplanton as well.

I also thank the research group that have taught me a lot on copepods, especially Lasse Eliassen and Even Garvang. For help with writing I would like to thank the writing group and everyone who have given me feedback and answered question. Thank you to Sine Hagestad, Amalie Gravelle, Carl Fagerlund, Julie Rydning, Simon Kline, Jan Heuschele, Torben Lode, Even Werner, Stein Fredriksen and everyone else at AKVA. I also want to thank Kyrre Grøtan for help with deadlines.

Finally, I want to thank my family for emotional and financial support while I wrote this thesis.

Table of contents

1 Introduction

Copepods and other zooplankton are important links between lower trophic levels (i.e., algae) and higher trophic levels (i.e., fish) ((Fransz et al., 1991)). They are often summarized as having a single food web position, namely as grazers. However, they inhabit several parts of marine food webs, acting as grazers, predators and detritivores (Mauchline, 1998). The feeding role of zooplankton varies with species but also has significant seasonal variation (Kiørboe, 2011). Food availability sets the foundation for the zooplankton food web and is affected by primary production as well as interactions within the microbial loop (Breton et al., 2021; Kenitz et al., 2017; Lundsør et al., 2022; Maar et al., 2002, 2004).

Estimating and understanding the food web position of copepod species through seasons helps further our understanding of the role of copepods in marine ecosystems. Food web position can be inferred through the measurement of stable isotopes, which provide an estimate of the weighted mean of its food throughout its life (Post, 2002; Tiselius & Fransson, 2016). Using stable isotope analysis of ^{15}N and ^{13}C allows the estimation of trophic level, or position in the food chain, and base source of carbon, allowing the estimation of food web position of organisms (Post, 2002).

Feeding biology of zooplankton

The feeding biology of zooplankton exists on a continuum between obligate herbivory and obligate carnivory. Where a zooplankton exists on this spectrum depends on organism traits (i.e., size, development stage, species traits) and food availability (Kiørboe, 2011; Litchman et al., 2013). Copepods and other meso-zooplankton are generally opportunistic (Serandour et al., 2023). However, species have different feeding modes (i.e., feeding current feeding, cruise feeding, ambush feeding) as well as prey selection (Fileman et al., 2007; Kiørboe, 2011; Kiørboe et al., 2009; Kjellerup & Kiørboe, 2012). Therefore, differences between species occur and the zooplankton community as a whole is affected by species composition in addition to other factors (Brito-Lolaia et al., 2022).

Food availability is affected by seasonality and depth. Zooplankton gets most of their energy directly from primary producers (Turner, 2004). The production of algae fluctuates with seasons, with a high production in spring, summer and autumn and low production in winter (Lundsør et al., 2022). Bursts of primary production lead to growth in the zooplankton

community of the North Sea in the spring and summer (Kiørboe & Nielsen, 1994). Protozooplankton such as Ciliates are also eaten and exist to a larger degree in the winter than the summer (Maar et al., 2002, 2004). Many copepods shift between eating proto-zooplankton and algae, leading to seasonal changes in trophic level (Castellani et al., 2008).

The zooplankton food web

Marine systems have an average of 4.0 trophic levels (Jake Vander Zanden & Fetzer, 2007), and most zooplankton have an omnivorous feeding strategy (Paffenhöfer, 1988). The food web in the North Sea and Skagerrak has a strong seasonal variation in zooplankton biomass following changes in primary productivity (Fransz et al., 1991; Kürten, Frutos, et al., 2013; Kürten, Painting, et al., 2013). Many copepods overwinter, while others are transported into the area (Fransz et al., 1991; Heath et al., 1999). Coastal areas have a higher production of herbivorous copepods, while the Skagerrak ridge has a higher production of protozooplankton due to more stratification (Maar et al., 2002, 2004).

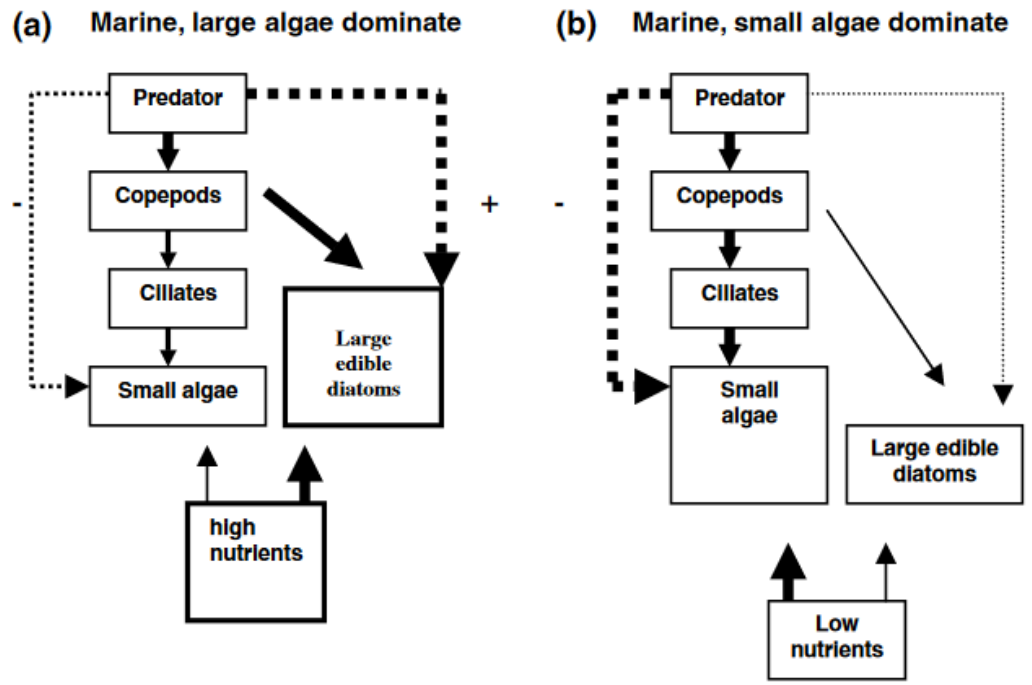

Figure 1.3: Conceptual presentation of direct (solid arrows) and indirect (dashed arrows) interactions in planktonic food webs. (a) Interactions in a marine system dominated by large algae. (b) Interactions in a marine system dominated by small algae. Copyright 2004, by Stibor et al.

Pelagic food chain length is complicated by interactions between copepods and microzooplankton (Fileman et al., 2010): Small phytoplankton increase food chain length because they are eaten by protists such as ciliates, which again is eaten by copepods, while large phytoplankton are more available for copepods to consume directly. Thus, copepods act as a switch between alternative food chain pathways, where they inflict grazing control on large phytoplankton and proto-zooplankton. The size of phytoplankton is mainly a consequence of nutrient availability, while grazing control from copepods and protists have different effects on different size classes (Boyce et al., 2015; Riegman et al., 1993; Stibor et al., 2004). Nutrient availability and phytoplankton assemblages vary with season as a response to several biotic (e.g. grazing pressure) and abiotic factors (e.g. stratification, nutrient availability) (Breton et al., 2021).

Stable isotopes and their use in food web analysis

Stable isotopes describe non-radioactive atoms by their nucleic count, determined by the number of neutrons and protons. For example, carbon isotope 13 has 7 neutrons in addition to their 6 protons and is written as ^{13}C. Due to its higher mass, ^{13}C moves slower than ^{12}C in chemical reactions, especially unidirectional reactions, as a consequence of Newton's second law[1] (Sharp, 2017, p. 13). For example, the absorption and incorporation of carbon dioxide into glucose during photosynthesis is slower for $^{13}CO_2$ than $^{12}CO_2$, leading to fewer ^{13}C in the eventual product glucose ($C_6H_{12}O_6$) than in the reactant carbon dioxide (CO_2). In this case the reactant (CO_2) is enriched in ^{13}C as it loses ^{12}C faster than it loses ^{13}C, while the product is depleted in ^{13}C as it gains ^{12}C faster than ^{13}C. This process is called stable isotope fractionation as the ratio of stable isotopes changes from reactant to product.

$$R(^{i}E\ ,^{j}E)_P = \frac{N(^{i}E)_P}{N(^{j}E)_P} \qquad (1)$$

The isotope-abundance ratio (R) of element E with isotope number i and j (i > j) in substance P. A briefer version is to write $R(^{i}E)$ instead of $(R(^{i}E, {}^{j}E)_P$. The ratio between ^{13}C and ^{12}C would be written as $R(^{13}C)$ and the ratio between ^{15}N and ^{14}N would be written as $R(^{15}N)$ (Brand et al., 2014).

The most common way to write a stable isotope ratio is relative to a recognised stable isotope standard using the delta notation (δ) in per mille units (‰). The per mille unit is relative deviation from a standard, meaning that an increase in 1 ‰ (VPDB) is an increase in 0.000011237 in R(^{13}C) because VPDB has a R(^{13}C) of 0.011237 (NOAA, 2023). In order to measure such small differences reliably it is also common to measure a sample with a known R(^{13}C) to correct for measurement inaccuracies which may be laboratory specific (Brand, 2014).

$$\delta = \left(\frac{R(^{i}E)_P - R(^{i}E)_{std}}{R(^{i}E)_{std}} \right) \cdot 1000\ (‰) \qquad (2)$$

The stable isotope delta notation (δ) describes the relative difference between the isotope number ratio R of isotope i of element E (Equation 1) of a sample P relative to the isotope number ratio R of a standard (std) in per mille unit (‰). For this thesis, stable isotope abundance ratios of ^{13}C is compared to the standard δ^{13}C (VPDB) ‰, while ^{15}N is compared to δ^{15}N (AIR) ‰, which can also be written as δ^{15}N or δ^{13}C. VPDB refers to R(^{13}C) in the standard Vienna Peedee Bellemnitella and AIR refers to R(^{15}N) in atmospheric nitrogen-gas (Brand et al., 2014).

Box 1.3: Reference materials for ^{13}C and ^{15}N

The PDB scale for carbon isotope 13 content is based on the ratio of ^{13}C to ^{12}C in a squid fossil from the Cretacean era called *Belemnitella americana* in the Peedee rock formation of Southern Carolina, USA. Due to its homogeneity in R(^{13}C) it was used by many of the first stable isotope labs as a reference material. After the exhaustion of this fossil, the commission on isotopic abundances and atomic weights (CIAAW) convened in Vienna to create a modified scale with the same 0-value as the PDB scale using a calcite compound called NBS19, chosen for its similarity to PDB and homogeneity in R(^{13}C). This scale is called Vienna PDB or VPDB and is used as a reference for δ^{13}C in this thesis (CIAAW, 2023).

The AIR scale for 15N is based on the stable isotope number ratio of ^{15}N to ^{14}N in atmospheric nitrogen. Atmospheric nitrogen is suitable due to its homogenous and stable ratio of ^{15}N (Junk & Svec, 1958).

In ecology, $\delta^{15}N$ and $\delta^{13}C$ can be used as indexes to create a two-dimensional map that reflects the positions of organisms in a food web (Deniro & Epstein, 1981; Peterson & Fry, 1987). On average, ^{15}N is enriched by 3.4 ‰ (sd=0.98) $\delta^{15}N$ per trophic level, while ^{13}C is conserved with a marginal increase of 0.39 ‰ (sd = 1.3) $\delta^{13}C$ (Post, 2002). There is also fractionation between different tissues and molecules: Lipids are depleted in ^{13}C by 6-8 ‰ $\delta^{13}C$ compared to the rest of the body due to fractionation during lipid synthesis (DeNiro & Epstein, 1977; McConnaughey & McRoy, 1979). Fractionation of $\delta^{15}N$ and $\delta^{13}C$ can vary: different taxa, body tissues and trophic roles have been observed to have different fractionations (Vanderklift & Ponsard, 2003). Stable isotopes might thus have some errors, and are most effectively used in combination with other methods (Caut et al., 2009; Martínez del Rio et al., 2009; Perkins et al., 2014).

Carbon 13 is conserved in trophic fractionation and measured $\delta^{13}C$ can be used to identify the source of carbon at the base of the food web (Post, 2002). $\delta^{13}C$ of sources vary due to differences in the uptake of CO_2, for example between C3 and C4 plants and different types of algae. Terrestrial sources and limnic plankton typically have a low value from -28 ‰ to -26 ‰ $\delta^{13}C$ (Meyers, 1994), while brown algae have a high value of -16 ‰ $\delta^{13}C$ (Fredriksen, 2003). Marine pelagic phytoplankton has been observed to vary from -20 ‰ $\delta^{13}C$ to -25 ‰ $\delta^{13}C$ during a spring bloom in a western Norwegian fjord, with a higher $\delta^{13}C$ at the peak of the bloom. This variation within the phytoplankton is mainly due to CO_2-recycling and taxonomic differences (Kukert & Riebesell, 1998). A copepod eating phytoplankton with ^{13}C varying from -20 ‰ $\delta^{13}C$ to -25 ‰ $\delta^{13}C$ integrates the ^{13}C of its diet over time, meaning that the ^{13}C of the bodies of the copepods, varies less than its source (Bearhop et al., 2004).

Aims

The overarching aim of this thesis is to examine the food web positions of the copepods of the Oslofjord through one year. In addition I quantify the relative contribution of different genera to the copepod community and predict the trophic level of the copepod community as a whole based on key genera. This can be summarized into the following aims.

1. To determine the trophic position of copepod genera in the Oslofjord.
2. To investigate the seasonal variation of trophic position and lipid content within important copepod genera.
3. To quantify the seasonal variation in trophic position of the zooplankton community through the combination of published biomass data and my own stable isotope data.
4. Investigate the effect of parasitism on trophic position and lipid storage in Calanus.

While aims 1 to 3 are described in detail in the following text, aim 4 is reported separately in a scientific publication (Appendix A: Eliassen et al., in review).

3 Materials and Methods

The practical method consists of the collection of zooplankton from a station as well as the preparation of samples for stable isotope analysis of $\delta^{13}C$ and $\delta^{15}N$. Zooplankton samples were collected with qualitative net hauls from the Oslofjord. I prepared isotope samples of copepod genera in a qualitative way as well. Stable isotope analysis was conducted by the CLIPT lab at UiO (*The ClIPT LAB - About the Lab*, 2023; *The CLIPT Stable Isotope Lab - YouTube*, 2023). $\delta^{15}N$ of Particulate Organic Matter (POM) was provided by the master student Tonje Storholt. I downloaded quantitative zooplankton biomass data for Släggö station from a database from the Swedish Meterological and Hydrological Institue (SMHI)(*SharkWeb*, 2023). Data was analyzed using the statistical software R (R, 2023; R-studio, 2023).

3.1 The IM2 station, Släggö station and surrounding area

Zooplankton used for stable isotope analysis was collected from the IM2 station (longitude 10.6282, latitude 59.6220), which is a 200 meter deep station located in the outer Oslofjord, at 4 km distance from the Drøbak sill. The Drøbak sill is 19 meter deep and separates the inner

Oslofjord from the outer Oslofjord. The Outer Oslofjord is connected to the Atlantic ocean through the Skagerrak area.

Släggö monitoring station (longitude 11.4346, latitude 58.2596) is used by swedish meterological and hydrological institute as a sampling station. They collected biomass data on zooplankton in the upper 25 meters at the 71 meter deep släggö station. I downloaded a dataset for zooplankton and presented biomass of important genera (*SharkWeb*, 2023).

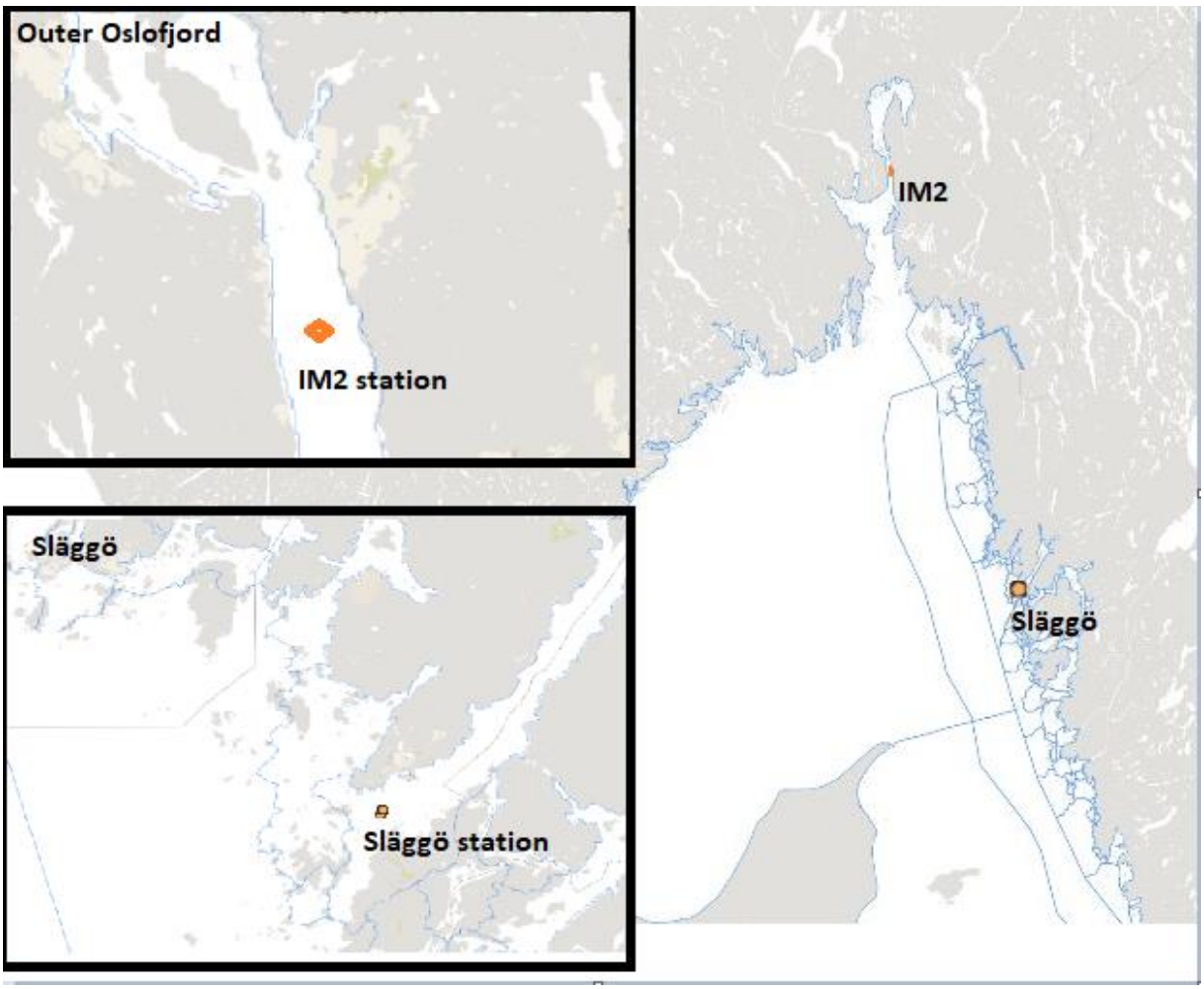

Figure 3.1: The position of the station IM2 and Släggö station is marked in orange on a map in sharkweb The IM2 station (sharkweb, 2023). The map was edited using paint.

3.2 Monthly zooplankton sampling.

Figure 3.2: The picture on the left is from the IM2 net haul site onboard Trygve Braarud. The picture on the right is a WP2 net (WP2-net, 2023).

We collected zooplankton samples for each month of 2022 except for July using the research vessel Trygve Braarud. The sampling was done in cooperation with the POICE crew and cruise leader Even Garvang. POICE is a research project which investigates the effects of parasitism on copepods ((*POICE*, 2021). We collected qualitative zooplankton samples with a WP2 net with a mesh size of 200 μm and an open cod end. A sufficient number of samples were collected from the water column (195-0 m) and collected into 50mL plastic bottles and conserved in a solution of filtered seawater and 1-5% Lugol acetate (Appendix D). The concentration of Lugol was estimated and adjusted based on the colour of the solution that the zooplankton sample was conserved in. Live zooplankton were killed by the Lugol, and since none were decapods or more complex animals, they are not covered by the animal protection laws of Norway (*Forskrift Om Bruk Av Dyr i Forsøk - Lovdata*, 2023).

I also prepared live zooplankton collected with a closed cod end in April (06.04-08.04) during a field course in BIOS4400, which was stored in seawater for a few hours before preparation. This data was also included in the dataset and time-series

3.3 The preparation of zooplankton for stable isotope analysis

Zooplankton was stored in Lugol acetate before preparation. The effect of Lugol on stable isotopes is minimal. Its effect is much less than other fixatives such as ethanol. A concentration of 10% has little effect on stoichiometry (Sano et al., 2020; Ventura & Jeppesen, 2009).

I organized stable isotope samples by month and taxon, the latter from group to species level, with highest species identification accuracy for copepods. In addition, a number of animals per capsule was decided for each species based on target dry weight and good statistical representation. A number of 30 individual animals per taxa per month was considered a sufficient number to obtain a significant statistical representation and is based on $\delta^{15}N$ variation (SD = 1.128) for individual *Calanus finmarchicus sl* (Eliassen et al., 2024, in review) (Appendix A and B).

The sample was inserted into a “6*4mm” or “8*5mm” tin capsule, which was placed on a 96 well plate. Sample dry weight was determined by subtracting tin capsule weight after and before addition of the isotope sample. Weight was measured using a Mettler Toledo xpr6ud5 Zaventem microbalance with precision of 0.5 μg. Sample dry weight varied from 100 μg to 3500 μg) according to advice from the CLIPT lab (*The ClIPT LAB - About the Lab*, 2023). Due to unexpected time constraints following asbestos sanitation of the stable isotope lab, the amount of samples and planning behind each sample was shortened. I prioritized zooplankton that were easy to pick, with the goal of getting an 11 month time series for *Calanus*, *Paraeuchaeta* and *Metridia* as well as data for a larger number species during the spring bloom and late summer. Labour-intensive species such as *Oithona similis* were down-prioritized. One isotope sample of Oithona would require approximately 300 individuals.

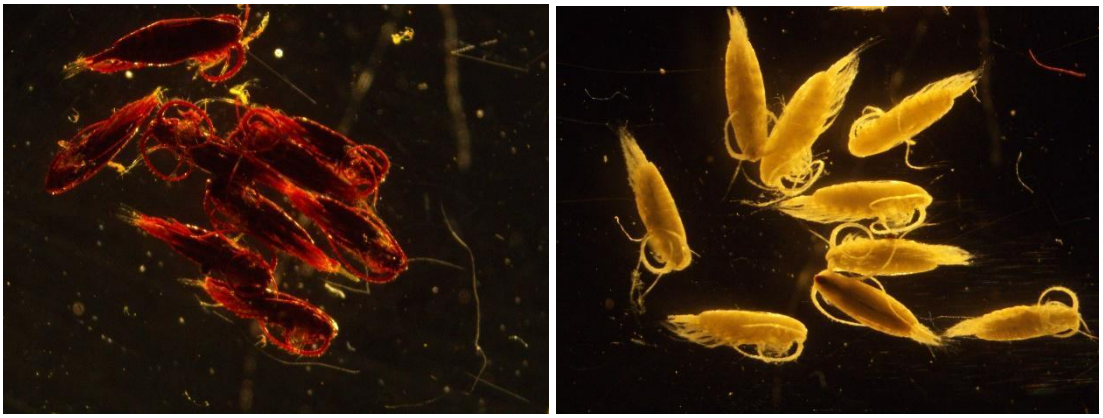

Figure 3.3: These two pictures are of 10 Lugol-fixated *Calanus* copepods before (left) and after (right) bath treatment with 0.1 M sodium thiosulphate $Na_2S_2O_3$.

Animals fixated in Lugol go through a linear shrinking effect which can be adjusted using a correction(Jaspers, 2009). Pictures were taken using a Nikon smz 1500 microscope with an inbuilt camera with magnification setting 1. This provided length and species verification. A 1 mm ruler was used as reference length and pictures were processed in Amscope (version: x64, 4.11.21462.20220922)The fixative Lugol was removed using 0.1 M sodium thiosulphate [$Na_2S_2O_3$] until the zooplankton had lost color (Fig. 3.3) and then washed with distilled water to remove any salt or halogen left that may degrade the silver cobalt oxide column of the elemental analyzer (Appendix C). After insertion into “6*4mm” or “8*5mm” tin capsules, samples weredried for 24 hours at 50 C in a drying cabinet, closed and sent in for analysis along with an ID, mass and well plate position sheet.

The live samples from BIOS4400 were prepared into 21 isotope samples. Unlike the other samples, these were not weighed and only distilled water was used for washing.

3.4 Stable isotope analysis

The stable isotope analysis was conducted by Senior Engineer William Martin Hagopian at the CLIPT stable isotope geochemistry lab at UiO (*The ClIPT LAB - About the Lab*, n.d.). The instruments used were a Thermo Fisher Scientific EA IsoLink IRMS System, consisting of an elemental analyser and an Isotope ratio mass spectrometer (Appendix C). For each run, 3 to 9 reference samples of JGLUT and POPPGLY were run and used to normalize the isotope values with the VPDB scale for ^{13}C, and AIR scale for ^{15}N. The analysis also provided data on the mass of nitrogen and carbon for each sample in microgram (µg), as well as the relative

stable isotope abundance ratio of $\delta^{13}C$ ‰ (VPDB) and $\delta^{15}N$ ‰ (AIR). The analysis of samples was successful for weights down to 100 µg dry weight, which is an exceptionally low mass for this analysis. The precision of the measurement was high with a standard deviation of 0.06 $\delta^{13}C$ and 0.07 $\delta^{15}N$.

3.5 Additional data: SMHI zooplankton biomass data and POM $\delta^{15}N$ stable isotope data

I downloaded a dataset for zooplankton biomass from the open source SMHI for the Skagerrak and Kattegat area from 2020 and 2021 ((*SharkWeb*, 2023). From this dataset, I selected biomass data (µg/m^3) of important zooplankton genera for the 71 meters deep coastal Släggö station for the upper 25 meters of the water column because it had the most complete biomass data (Appendix E).

Masterstudent Tonje Storholt collected water samples from 5 stations in the outer Oslofjord from 3 to 4 meters depth on the 13th of May, 2nd of June and 30th of June 2022. They were used for 24-hour ^{13}C-incubation experiments and filtered through glass fiber filters ((Storholt, 2023). I used the $\delta^{15}N$ data of her filter-samples to get an overview of the range of trophic level of the filter content in order to estimate the $\delta^{15}N$ of the pelagic base of the food chain.

3.6 Data analysis

Stable isotope data was analyzed in R (version 4.2.2) (R,2023; R-studio, 2023). The analysis consists of simple statistical measures (i.e., mean and standard deviation), statistical models (i.e., linear models, linear mixed models) and estimations of trophic level and lipid content. The dataset contain isotope measurements of $\delta^{15}N$ and $\delta^{13}C$, mass measurements of C and N as well as sample background data (i.e., date of collection, taxa, weight) (Appendix E). In addition, SMHI's biomass data from Släggö station and Tonje's POM measurements were applied. Data was presented visually using the ggplot package in R.

Estimations of trophic level:

Trophic level is estimated based on Post's (2002) estimates of trophic fractionation as well as the $\delta^{15}N$ of an obligate herbivore or direct measurements of autotrophs. $\delta^{15}N$ fractionates by 3.4 (SD = 1.0) ‰ $\delta^{15}N$ per trophic level and $\delta^{13}C$ by 0.4 (SD=1.3) ‰ per trophic level (Post, 2002).

I decided to choose the herbivore with the lowest $\delta^{15}N$ integrated over a longer time interval as a baseline trophic level 2.0 for the zooplankton community in accordance with Post's (2002) recommendation. *Temora longicornis* is the most suitable species available for this method as it has little temporal and spatial variation in its diet, which for the most part consists of cyanobacteria (Serandour et al., 2023). I also looked at POM-values to assess the validity of the baseline estimation.

Lipid correction

It is common to correct the $\delta^{13}C$ of an organism through lipid correction in order to reduce bias. Since lipids do not have nitrogen, the carbon to nitrogen mass ratio, or C:N ratio of the entire body can be used to correct $\delta^{13}C$ based on an empirical relationship between lipid content and C:N ratio. This can be done through the following empirical equations for lipid correction in aquatic animals (Post et al., 2007a):

$$\%L = -20.54 + 7.24 \cdot \frac{C}{N} \quad (3)$$

The fraction of lipids (L) in percentage (%) of dry mass is calculated using a linear equation with intercept -20.54 and slope 7.24 per C:N increase. This equation is based on aquatic animals with a C:N ratio between 3 and 7.

$$\Delta\delta^{13}C = -0.47 + 0.13 \cdot \%L \quad (4)$$

Change in $\delta^{13}C$ is calculated with a linear equation with intercept -0.47 and slope 0.13 per %L. %L is from equation 3.

$$'\delta 13C = \delta 13C + \Delta\delta 13C \quad (5)$$

Lipid correct $\delta^{13}C$ ('$\delta^{13}C$) is the measured value of $\delta^{13}C$ added with the change of $\delta^{13}C$ ($\Delta\delta^{13}C$) based on the C:N dry mass ratio and equation 3 and 4.

Linear mixed effect model:

Linear mixed effect models predict the observed measurements using random and fixed effects. These models are useful for hierarchical data, where variables are dependent on each other (Bates et al., 2015).

I used this model to predict the effect of body mass (log(Nitrogen mass)) and genus on δ^{15}N using the "lmer" function in the lme4 package (Bates et al., 2015). Genus is a grouping variable and has a random effect, while body mass has a fixed effect. I made an interactive model and an additive model with genus and body mass and decided to use the model with the lowest AIC-score.

AIC-score:

An Akaike Information Criteria score or AIC-score balances between the complexity of a model and its ability to predict the observations accurately . Scores of models that use the same data are compared with each other and the lowest score has the best quality (J. B. Johnson & Omland, 2004).

Time series models

SMHI's Släggö zooplankton biomass data was combined with taxa-specific mean δ^{15}N values to construct a predicted δ^{15}N signature of the zooplankton biomass according to the following equation:

$$\sum\left(\left(\frac{Genus\ biomass}{Total\ biomass}\right) \cdot\ \delta^{15}N_{(Genus)}\right) \qquad (6)$$

SMHI collected zooplankton biomass data from a coastal station called Släggö on the Swedish west coast. A depth interval of 0-25 meters out of 71 meters was sampled in 2020 and 2021 and curated into a dataset by SMHI (*SharkWeb*, 2023).

Equation 6 was used to estimate δ^{15}N for day of year each SMHI sampling date by producing weighted mean based on the biomass of a genus from the Oslofjord. *Evadne* and *Penilia* was assigned the δ^{15}N value from the August isotope sample *Evadne* due both being cladoceran and filter-feeders ((Katechakis & Stibor, 2004), with a value of 5.94 ‰, which was the lowest isotope measurement in my dataset.

4 Results

I prepared a stable isotope and atomic mass dataset of nitrogen and carbon, which contain 343 stable isotope data values, with over 30 taxa-specifications and approximately 3500 individual zooplankton. Of this dataset I present the stable isotope signatures of 12 taxa including approximately 3000 individuals; 7 copepod genera which have data for several months (Fig. 4.) and five additional taxa which are important contributors to zooplankton biomass (fig. 4.1). Complementary to this dataset are SMHI zooplankton biomass data and POM $\delta^{15}N$ signatures from another master student.

4.1 Seasonal zooplankton biomass; The SMHI zooplankton monitoring dataset

The biomass ($\mu g/m^3$) of the 9 most frequently measured taxa in the upper layer at the Släggö station consist of 6 calanoid copepod genera, the cyclopoid copepod genus *Oithona* and 2 cladoceran genera. Biomass is lowest in January at 244 $\mu g/m^3$ and highest in May at 4541 $\mu g/m^3$, a difference by a factor of 18.6. The relative contribution of each taxa also varies throughout the year. The cladocerans *Evadne* and *Penilia* contribute more than half the biomass in May, August and September (Appendix E).

There is a high variation between measurements and the prediction, meaning that there is a high degree of patchiness or random effect between collections. *Acartia*, *Temora* and *Pseudocalanus* have a peak of biomass in May, while *Paracalanus*, *Evadne* and *Oithona* peak in the summer.

Biomass is dominated by high mass of *Penilia* and *Evadne* during their peaks in June and September. There are fewer measurements of *Penilia* and *Evadne* than other genera. Other genera like *Calanus* and *Centropages* have a stable biomass during the summer.

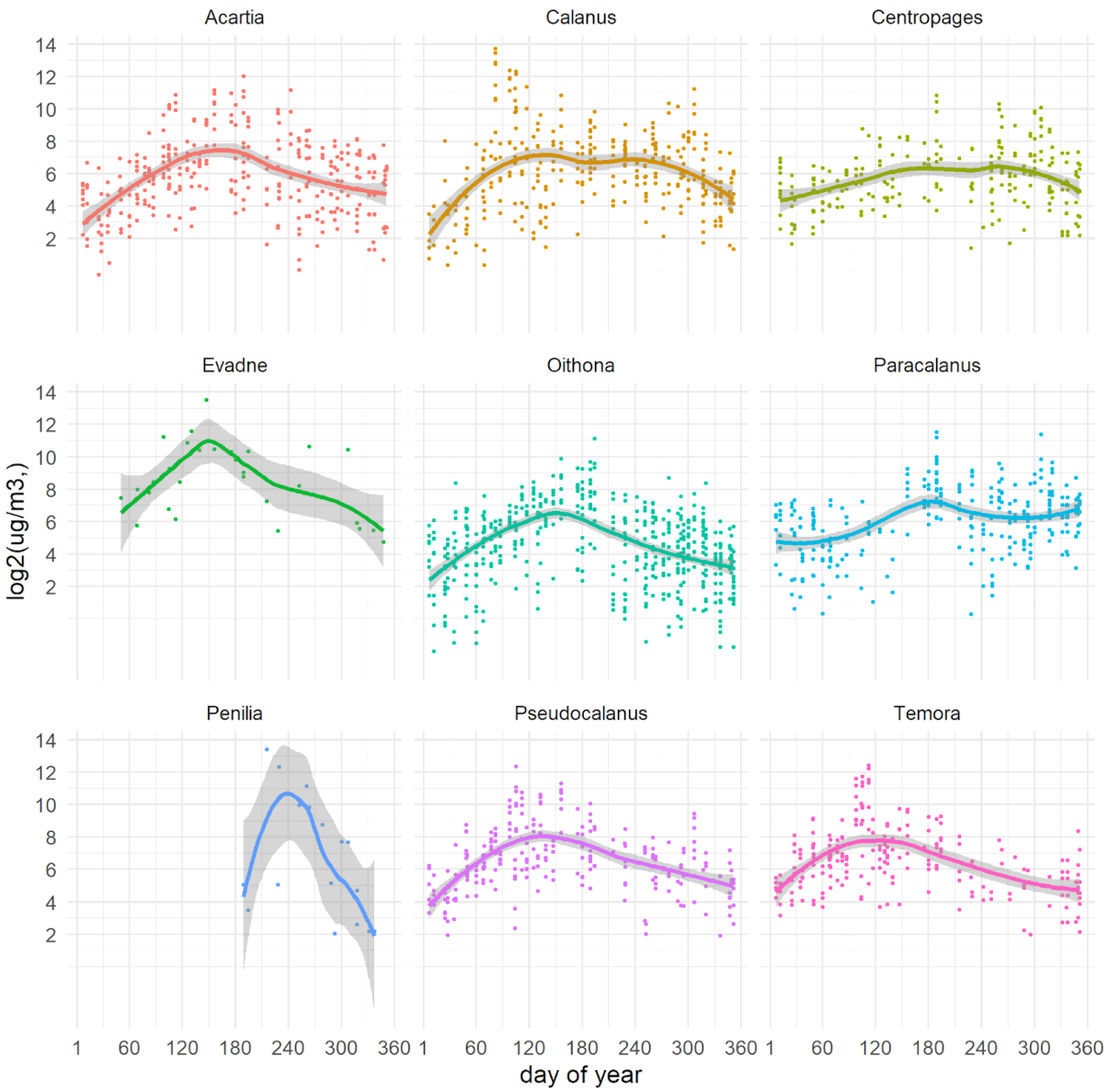

Figure 4.1: Concentration of biomass per cubic meter vs day of year of 9 taxa for the upper 25 meters at the Släggö station. The package ggplot2 was used. Geom_smooth with default LOESS regression was provides a lined prediction, with shadowed 95% confidence intervals.

4.2 Estimating baseline $\delta^{15}N$ from POM and *Temora*

The $\delta^{15}N$ of seston or particulate organic matter (POM) has an interquartile range of 5.7 ‰ to 7.8 ‰, while the baseline $\delta^{15}N$ estimated from *Temora* is between 4.3‰ to 6.3‰. These two estimates have a difference of 1.5 ‰, which is comparable to half a trophic level.

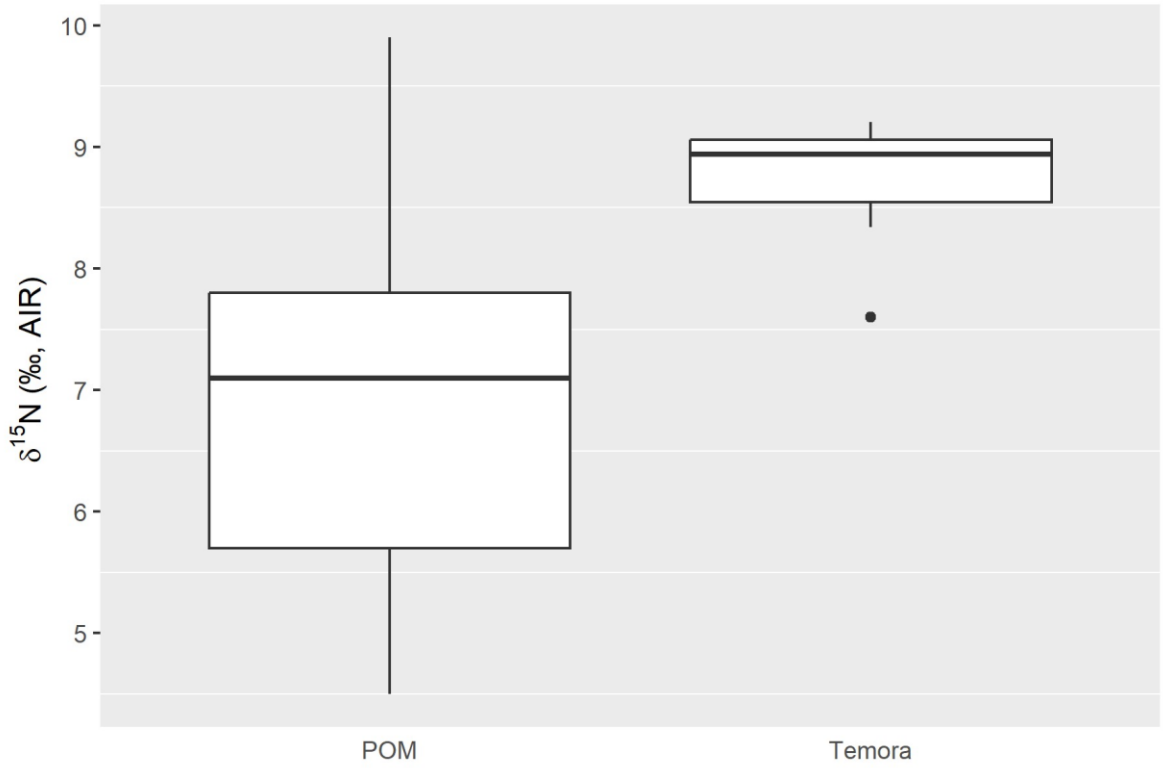

Figure 4.2: Boxplot of $\delta^{15}N$ (% AIR) values of POM from filter sample content and measurements of *Temora* isotope samples. Filter samples from locations in the Oslofjord and used in an incubation experiment were analyzed through stable isotope analysis to obtain $\delta^{15}N$ (% AIR) values.

Filtered sample had $\delta^{15}N$ measurements that overlapped with the lowest $\delta^{15}N$ measurements among copepods: Filter samples had an interquartile range from 5.7 ‰ to 7.8 ‰ with a median of 7.1 ‰ (Fig. 4.2), which overlaps with the lowest zooplankton $\delta^{15}N$ such as *Evadne* and Appendicularia (Fig. 4.4). The $\delta^{15}N$ of filtered particles varies temporarily and spatially with an expected standard deviation of 1.4 ‰ and a mean of 6.9 ‰. With a baseline of 6.9 ‰ (± 1.4 ‰ (SD)) and a trophic discrimination factor of 3.4 ‰ (± 1.0 ‰ (SD)), the consumer of this material would have an expected $\delta^{15}N$ value of 10.3 ‰, which is higher than the mean $\delta^{15}N$ of *Centropages*, *Acartia* and *Temora* (Fig. 4.3).

Temora has the lowest $\delta^{15}N$ with its mean value of 8.74 ‰. The expected baseline with the assumption that the trophic fractionation of 3.4 ‰ (±1‰ SD) is from 4.3 ‰ to 6.3 ‰ and is for the most part below the interquartile range of the filter samples, but is mostly within the total range of 4.5‰ to 9.9‰ of the filter-samples.

4.3 Stable isotope values of copepod genera and two other taxa:

The stable isotope measurements of the 7 genera *Paraeuchaeta, Metridia, Chiridius, Calanus, Centropages, Acartia and Temora* represented the majority of the stable isotope dataset, being 242 out of 343 samples of the samples and 2215 out of 3500 of the individuals (Appendix D and E). Some other important taxa that were sampled more sporadically due to time constraints are also presented.

I plotted $\delta^{13}C$ vs $\delta^{15}N$ in order to gain a two-dimensional overview of the trophic position of the genera. $\delta^{13}C$ indicates the source of the organism's carbon and lipid content (Post et al., 2007a), while $\delta^{15}N$ is a proxy for trophic level (Post, 2002). Mean and 95% confidence intervals of genera are presented as name tags and lines. The number of animals per sample varied from a minimum of 1 in *Paraeuchaeta* to 50 in *Acartia*, but is for the most part 10 or 15 animals per sample.

The trophic map gather copepod genera into two main groups, characterized by their $\delta^{15}N$ values: The lower trophic group of *Temora, Centropages, Acartia* and *Calanus* with mean $\delta^{15}N$ ranging from 8.74 ‰ [7.96, 9.52] to 10.26 ‰ [9.96, 10.56], and the higher trophic group of *Chiridius, Metridia* and *Paraeuchaeta* with a mean ranging from 12.51 ‰ [12.17, 12.85] to 13.71 ‰ [13.45, 13.97]. The smallest difference in mean $\delta^{15}N$ between the two groups is 2.25 ‰ (0.66 TL) between *Calanus* and *Chiridius*.

Overall, there is an equally high absolute variation of $\delta^{15}N$ and $\delta^{13}C$ of approximately 8 ‰ in measurements, but a higher variation in mean $\delta^{15}N$ than $\delta^{13}C$ of copepod genera. Mean $\delta^{15}N$ has a difference of 4.97 ‰, between *Temora* and *Paraeuchaeta*, which is higher than variation in $\delta^{13}C$, which is 1.69 ‰ between *Acartia* and *Chiridius*. Moreover, variation in $\delta^{13}C$ is greater than variation in $\delta^{15}N$ within a genus: Standard error for $\delta^{13}C$ is greater than standard error of $\delta^{15}N$ for all 7 genera and the ratio between the standard error of $\delta^{13}C$ and $\delta^{15}N$ is between 1.43 to 1.53 for all genera except *Calanus*, which has a ratio of 3.5.

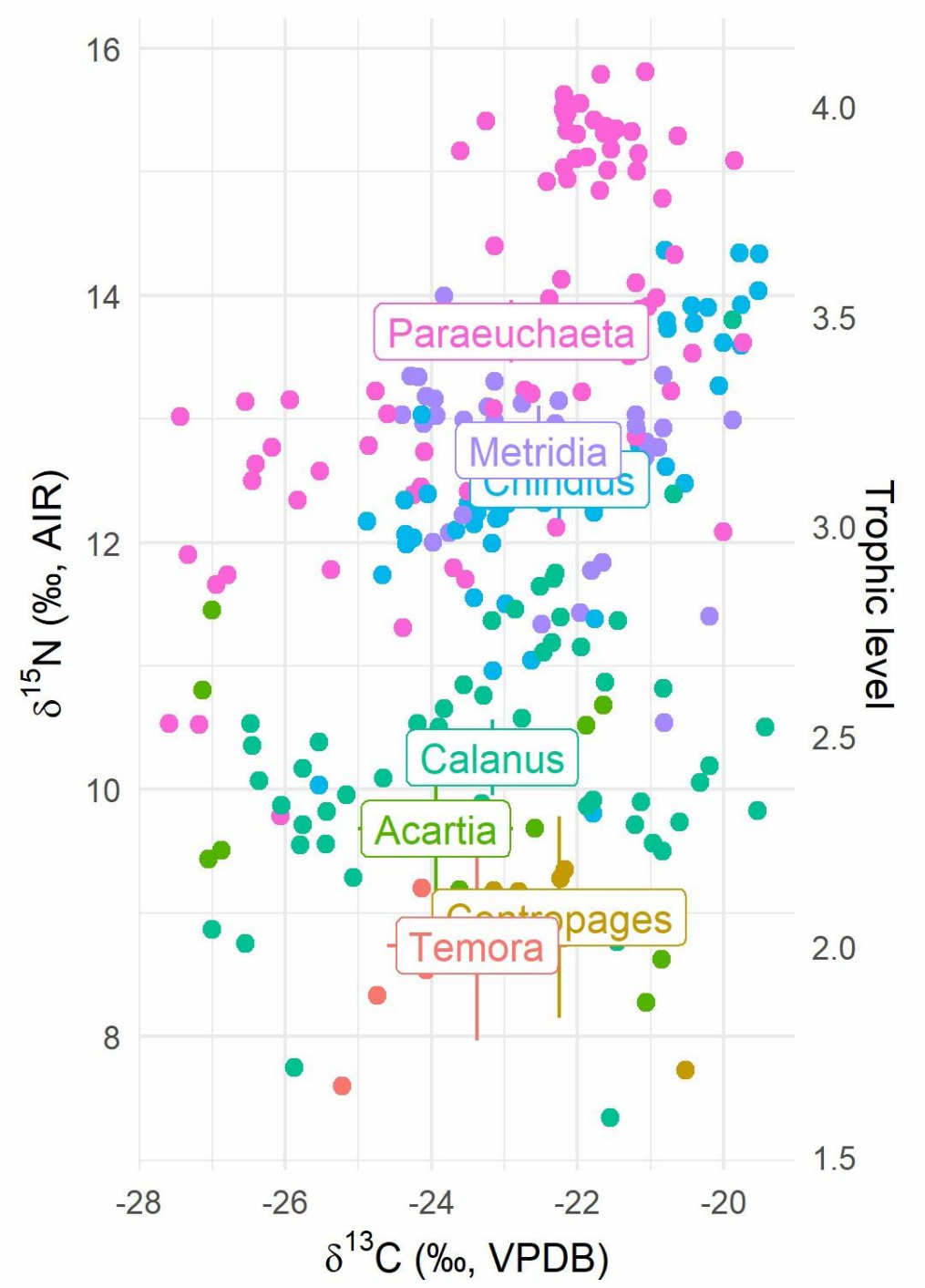

Figure 4.3: Stable isotope measurements of $\delta^{13}C$ (‰ VPDB) and $\delta^{15}N$ (‰AIR) from time-series data of 7 genera: Dots represent measurements of samples while tags and lines represent mean values and 95% confidence intervals. The labels represent the mean. Confidence intervals are small enough to be covered for labels. The second y-axis shows estimated trophic level based on a fractionation of 3.4 ‰ $\delta^{15}N$ per trophic level. Trophic level 2 is centered on the mean $\delta^{15}N$ of *Temora*.

Relative stable isotope abundance ratios of samples from other important contributors to the biomass of the zooplankton community (Fig 4.1) are presented here. They were prepared from fewer monthly net hauls. I did not calculate a mean and standard error for these samples as the sample number is too small and because they do not represent the variation over longer time-periods.

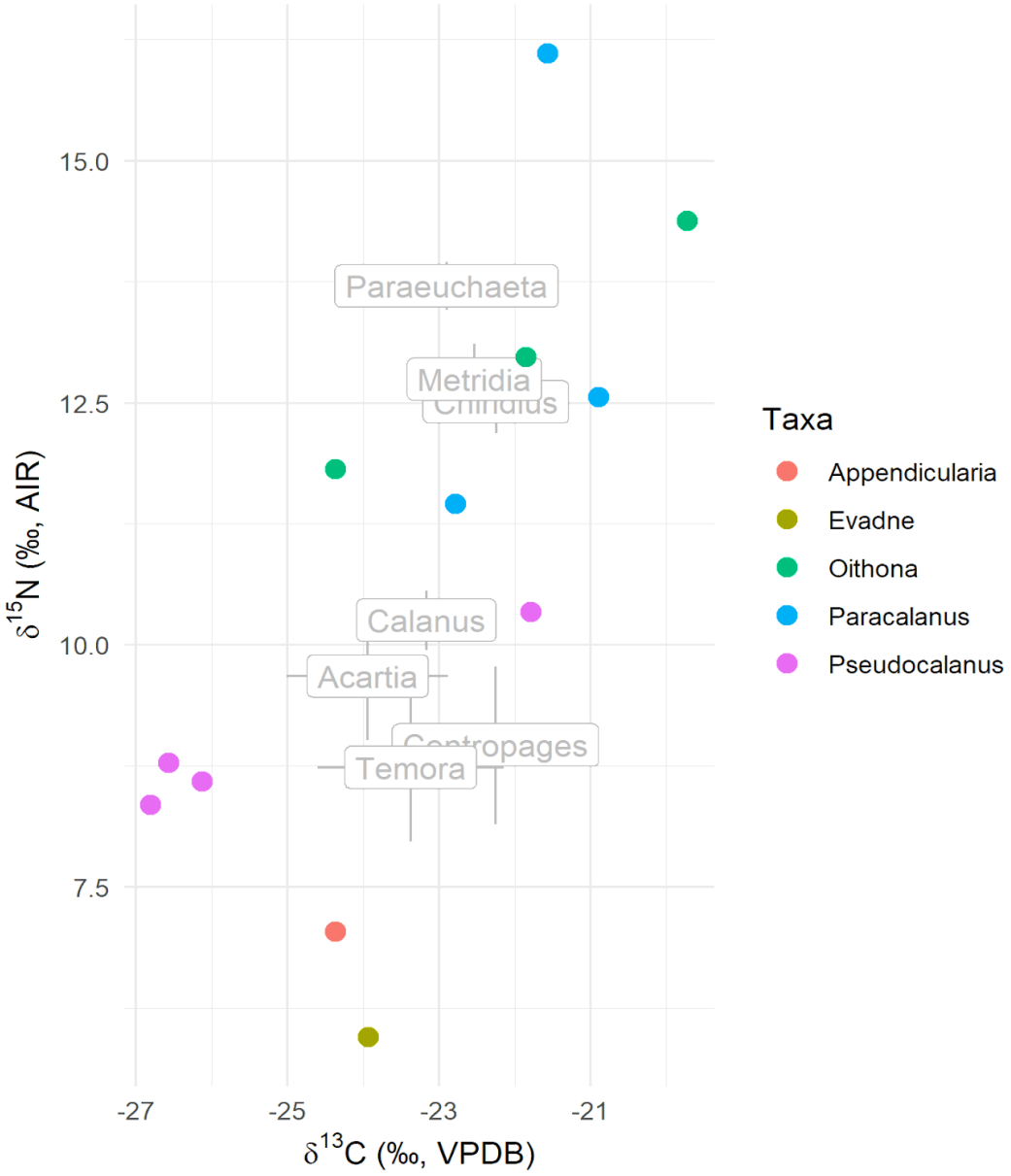

Figure 4.4: Stable isotope data of $\delta^{13}C$ (‰ VPDB) and $\delta^{15}N$ (‰AIR) from samples of 5 taxa, the copepod genera *Paracalanus, Pseudocalanus* and *Oithona*, the class *Appendicularia* and the cladoceran genus *Evadne*. Mean and confidence intervals for measurements of the other 7 genera (Fig 4.3) is presented in grey.

Three taxa are comparable with the two groups formed from the time series data (Fig. 4.3). *Paracalanus* and *Oithona* cover the higher trophic group despite their small size, while *Pseudocalanus* overlaps with the lower trophic group. Two outlier taxa: *Evadne* and *Appendicularia* have a $\delta^{15}N$ that is lower than the samples from the time-series data (Fig. 4.3) and *Evadne* has the lowest sample in the dataset (Appendix E). Both *Evadne*, which consisted of 40 animals in one sample and *Appendicularia* of 8 animals were from the August zooplankton collection.

4.4 Modelling seasonal trophic level of the zooplankton community

I combined $\delta^{15}N$ values of zooplankton collected in the Oslofjord with the biomass of zooplankton from the SMHI dataset in order to estimate average $\delta^{15}N$ of the Släggö zooplankton community for a yearly cycle. There is an estimated high $\delta^{15}N$ value of 11 ‰ in the zooplankton community in the winter and a low $\delta^{15}N$ of 8.5 ‰ in the summer, a difference which corresponds to 1 trophic level. Estimates of $\delta^{15}N$ vary depending on the presence of *Evadne* and *Penilia* in the summer months.

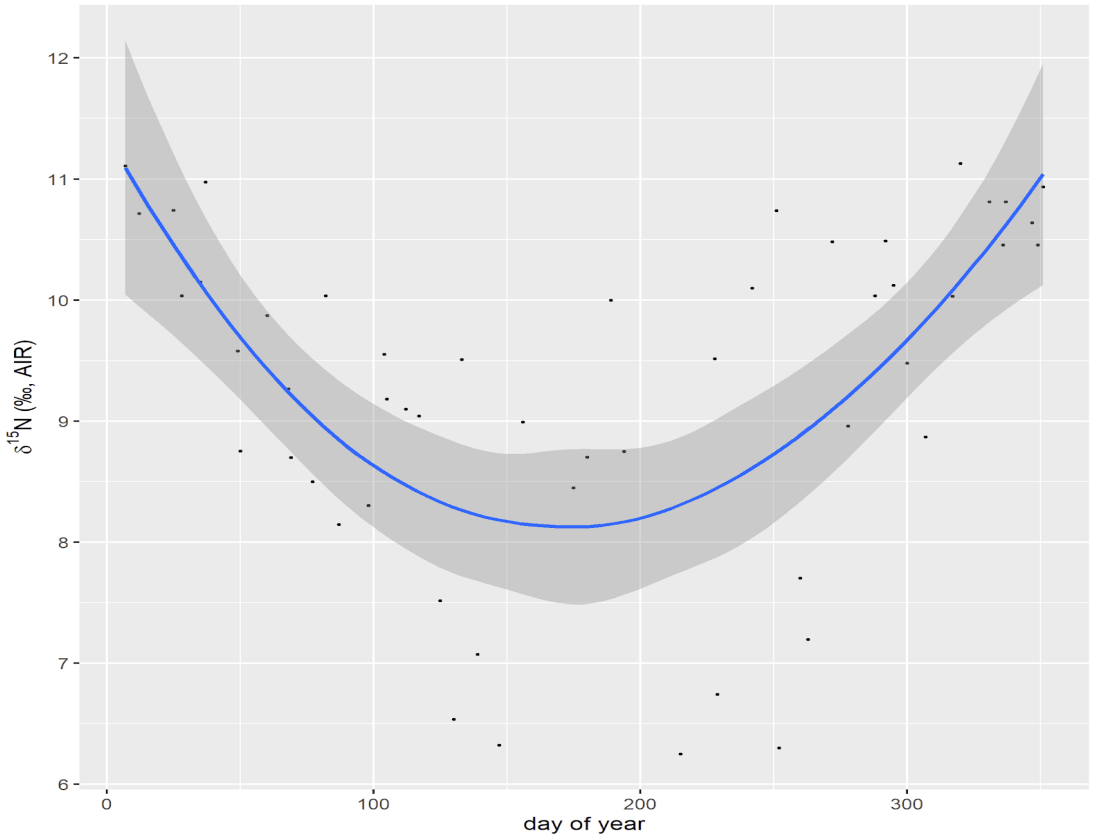

Figure 4.5: $\delta^{15}N$ (‰AIR) modelled from SMHI's biomass data of the top 9 genera of the upper 25 meters at Släggö station combined with mean $\delta^{15}N$ (‰AIR) values of genera from my dataset. Mean $\delta^{15}N$ (‰AIR) of the zooplankton community was calculated using equation 6 for each day of year. LOESS regression was used to fit a trend line with shaded confidence intervals.

Estimated $\delta^{15}N$ was at its highest in the beginning and end of the year and at its lowest in the middle of summer. Estimated $\delta^{15}N$ ranged from approximately 8.3 ‰ to 11.1 ‰. High biomass of *Evadne* and *Penilia* caused low estimated $\delta^{15}N$ during their peaks and also a broader confidence interval.

4.5 Variation of trophic level by size

The linear mixed effect models show a positive correlation between size and $\delta^{15}N$, but also significant different effects from genus that is more significant than the effect of size. Overall, a 10-fold increase in body mass is expected to have a 0.85 ‰ $\delta^{15}N$ increase for the additive model. The additive model had the lowest Akaike Information Criterion (AIC) is presented graphically (Fig 4.6). Tables are included in appendix D.

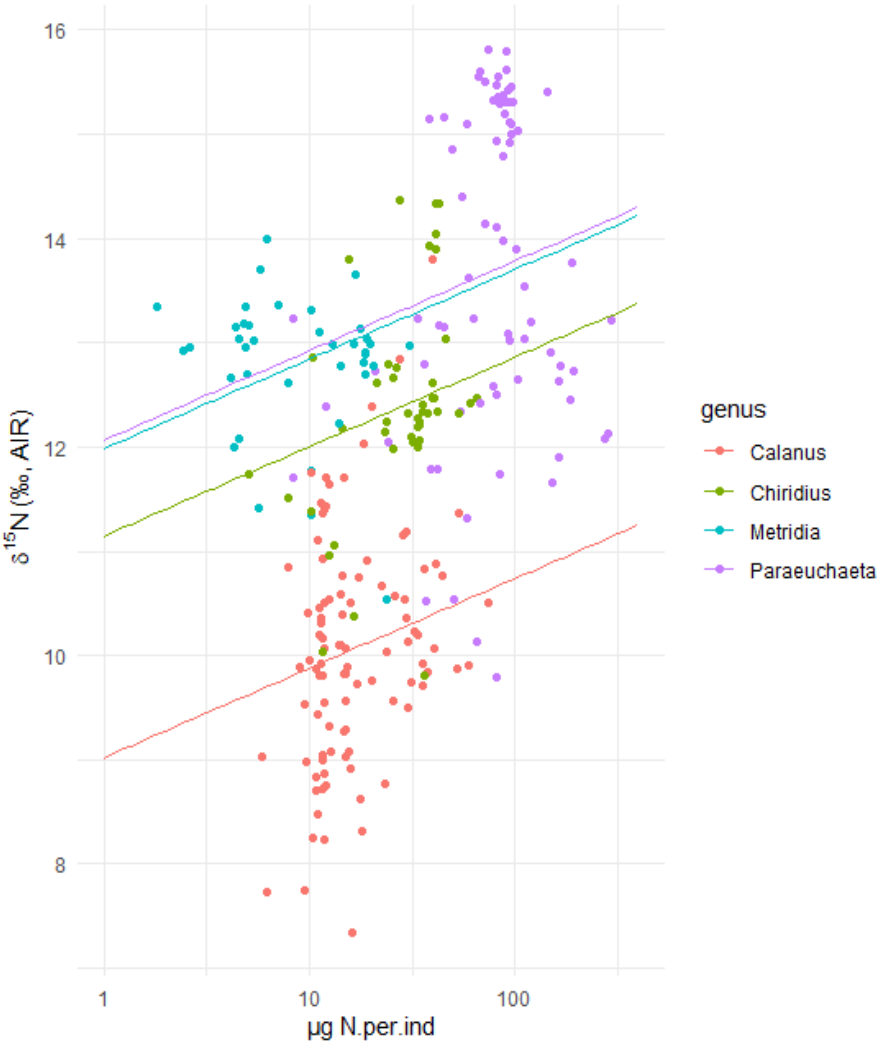

Figure 4.6: Trophic level represented by $\delta^{15}N$ ‰ (AIR) vs nitrogen mass per animal of the four genera *Calanus*, *Chiridius*, *Metridia* and *Paraeuchaeta*. Multileveled linear additive models were created using lmer based on genera and nitrogen mass per animal.

The animals of each genus had a varying range in size with a total range of 1.7 to 300 µg nitrogen per individual, though there is overlap between all genera. There is a significant predicted effect from size on $\delta^{15}N$. However, genus can predict more of the variation of $\delta^{15}N$. Overall, there is a high spread in $\delta^{15}N$ data compared to size, meaning that correlation between size and $\delta^{15}N$ is low.

The lowest AIC-score was for the additive model lme1 by an AIC-difference of 1.73 and is therefore equally successful as the interactive model. Based on the principle of increasing parsimony or reducing complexity of explanations, the additive model is the better model. The additive model predicted an increase in 0.85 $\delta^{15}N$ per 10-fold increase in mass of nitrogen, which is equivalent to a quarter of a trophic level: A theoretical increase from 1.7 µg to 300 µg/n.per.animal in size would lead to a predicted increase of 1,9 ‰ $\delta^{15}N$, which is approximately half a trophic level.

4.6 Seasonal variation in $\delta^{13}C$ and $\delta^{15}N$

There is significant seasonal variation in $\delta^{13}C$ and $\delta^{15}N$ within each genus (Fig. 4.7-4.9). I present the monthly variation in $\delta^{13}C$ and $\delta^{15}N$ together, then $\delta^{13}C$ with lipid-adjusted values and $\delta^{15}N$ vs month.

Figure 4.7: Monthly average $\delta^{13}C$ (‰ VPDB) and $\delta^{15}N$ (‰AIR) from time-series data of selected genera. Each point is marked with the month the data was collected and was connected using. A full year (Jan.-Nov.) time-series was prepared for *Calanus*, *Paraeuchaeta*, *Metridia* and *Chiridius*, while shorter samples of shorter intervals were prepared for *Temora*, *Centropages* and *Acartia*.

Time series data show significant variation in mean $\delta^{15}N$ and $\delta^{13}C$ of genera between monthly zooplankton collections from the IM2 station. Variation is approaching a cyclical pattern for 11-month time series (i.e., *Calanus, Chiridius, Metridia, Paraeuchaeta*), but not for genera sampled in a shorter interval (i.e., *Acartia, Centropages, Temora*). The change in $\delta^{13}C$ is different for each genus, while $\delta^{15}N$ is higher in the winter season and generally lower in the spring and summer for the 11-month time series.

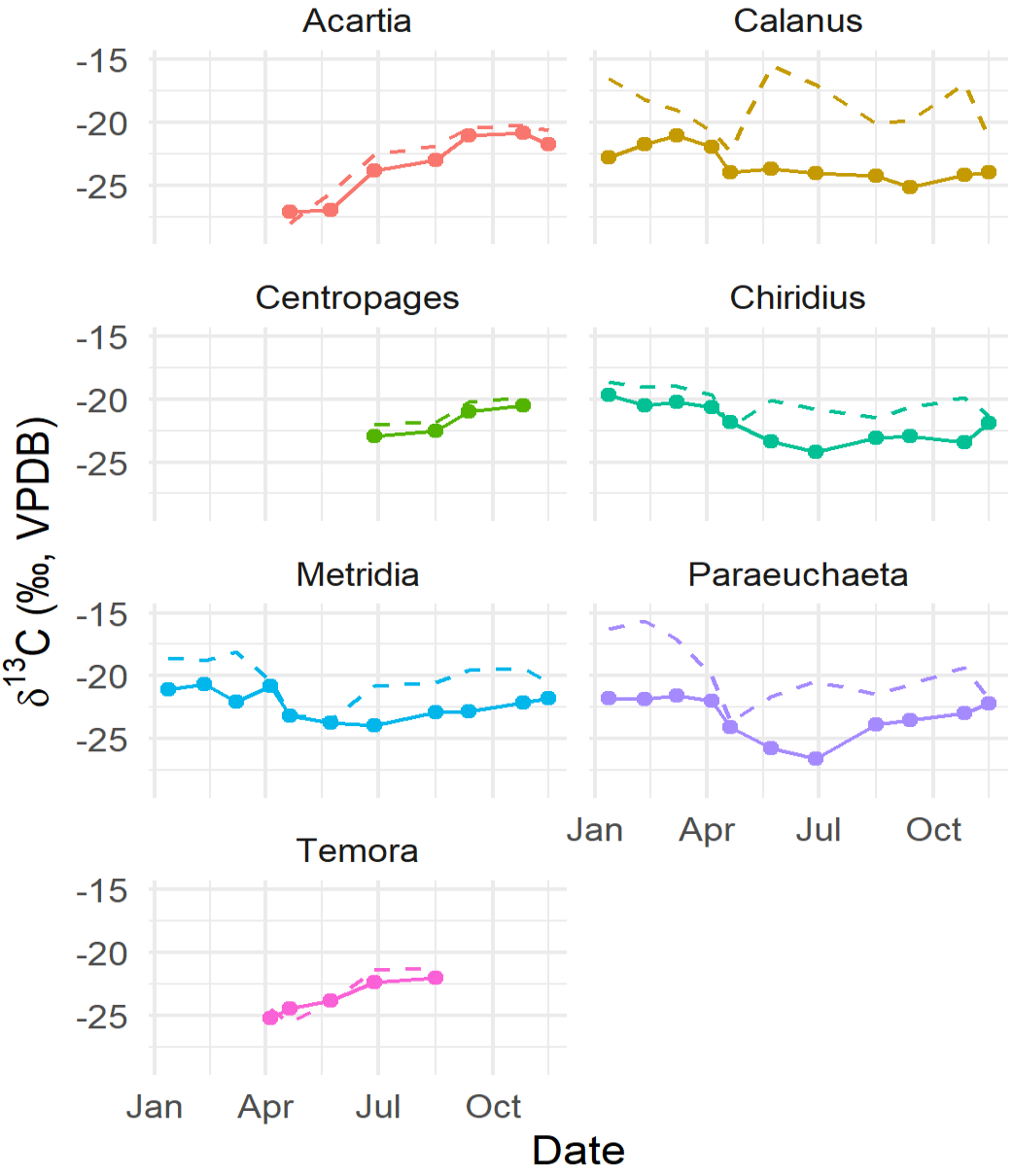

Figure 4.8 $\delta^{13}C$ (‰ VPDB) vs Date from time series data of selected genera. Geom_path was used to link each month to each other. A full year time-series was prepared for *Calanus, Paraeuchaeta, Metridia* and *Chiridius*, while shorter time series were prepared for *Temora, Centropages* and *Acartia*. Lipidadjusted $\delta^{13}C$ was added as a dashed line and was calculated using C:N ratio and equation 4-6 (Post, 2007).

Lipid-adjusted $\delta^{13}C$ is similar to measured $\delta^{13}C$ for *Temora*, *Centropages* and *Acartia*, but significantly different for *Metridia*, *Calanus*, *Paraeuchaeta* and *Chiridius*. Lipid adjusted $\delta^{13}C$ is at its lowest value in April for all genera, while measured $\delta^{13}C$ is at its lowest during summer or autumn for *Calanus*, *Metridia* and *Paraeuchaeta.* Lipid-adjusted $\delta^{13}C$ is above -23.5 ‰ for *Metridia*, *Calanus*, *Chiridius*, *Centropages* and *Paraeuchaeta*. The minimum measured values for *Temora* and *Acartia* were -25.2 ‰ and -27.1 ‰ respectively. The variation was high for all genera, but is most significant for *Acartia*, which moves from a minimum of -27.1‰ in April to a maximum of -20.9 ‰ in August, which is comparable to lipid-adjusted *Calanus* values for August.

The lipid correction acts as a proxy for lipid content where a higher correction means higher lipid content. *Calanus* had the highest average lipid content (Fig. 4.10). Lipid content is lowest in April and highest in the summer and winter.

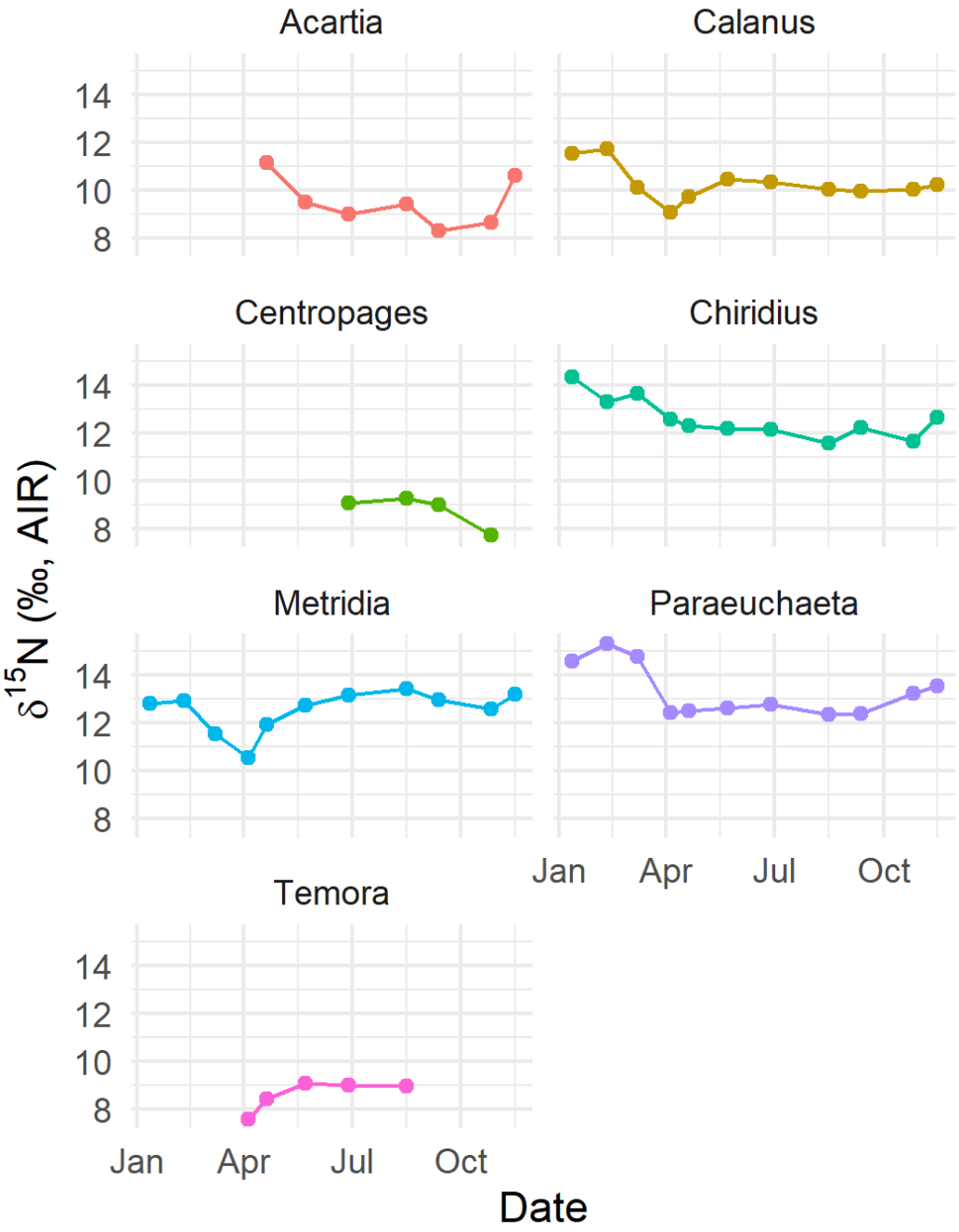

Figure 4.9: Trophic level through $\delta^{15}N$ (‰AIR) vs month of zooplankton sampling for seven selected genera.

The difference between maximum and minimum monthly mean $\delta^{15}N$ varied from 2.64 ‰ to 2.92 ‰ for the full time-series and from 1.47 ‰ to 2.85 ‰ for the limited time series. This difference is comparable to the differences observed between the genera (Fig. 4.3). The lowest differences (<1.7‰) was in *Temora* and *Centropages*, while larger differences (>2.5‰) were observed in *Calanus*, *Chiridius*, *Metridia*, *Acartia* and *Paraeuchaeta*. All

genera have a high value in winter (Jan- Mar) and a lower value in April, though there are different trajectories throughout summer and autumn for the genera.

Calanus and *Metridia* had the highest $\delta^{15}N$ value in January and February and the lowest in April, decreasing by 2.64 ‰ and 2.36 ‰ respectively. A similar trend in this time period was also present for *Paraeuchaeta* and *Chiridius*. Late spring and summer (May-Aug) saw an increase for *Calanus*, where it remained stable until the end of the year. *Metridia* had the highest value in the summer.

Acartia had a $\delta^{15}N$ above 11 ‰ in April and November and below 9 ‰ in September and October. In contrast, *Temora* had its lowest two $\delta^{15}N$ means in April of 7.6 ‰ and 8.4 ‰ and a stable value of 9 ‰ for the rest of the summer.

4.7 Lipid content by genera

Lipid content is higher in copepods with longer life cycles such as *Calanus*, *Paraeuchaeta*, *Metridia* and *Chiridius*. Lipid content of *Calanus* and *Paraeuchaeta* varied the most across the seasons, with lowest content during the zooplankton bloom of April and May and highest content during the summer before decreasing through the winter.

The mean lipid content of different copepod genera varied from 5% to 40 %, with highest content for *Calanus* and *Paraeuchaeta*. The genera *Temora*, *Acartia* and *Centropages* had the lowest lipid-content, with mean values below 10% while Chiridius and Metridia had intermediate lipid content with mean values between 15% and 20%. Width of confidence intervals indirectly reflect sample size differences: Genera with fewer animals per sample have more samples and a lower confidence interval.

The mean fractionation of $\delta^{13}C$ differentiates by less than 2 ‰ between the seven genera. Lipid fractionation according to equation 4 would entail a decrease of 1.3 ‰ $\delta^{13}C$ per 10% increase in lipid content. This is higher than the observed reduction in $\delta^{13}C$ from *Centropages* to *Calanus*. *Acartia* had the lowest mean $\delta^{13}C$ both before and after lipid content reduction.

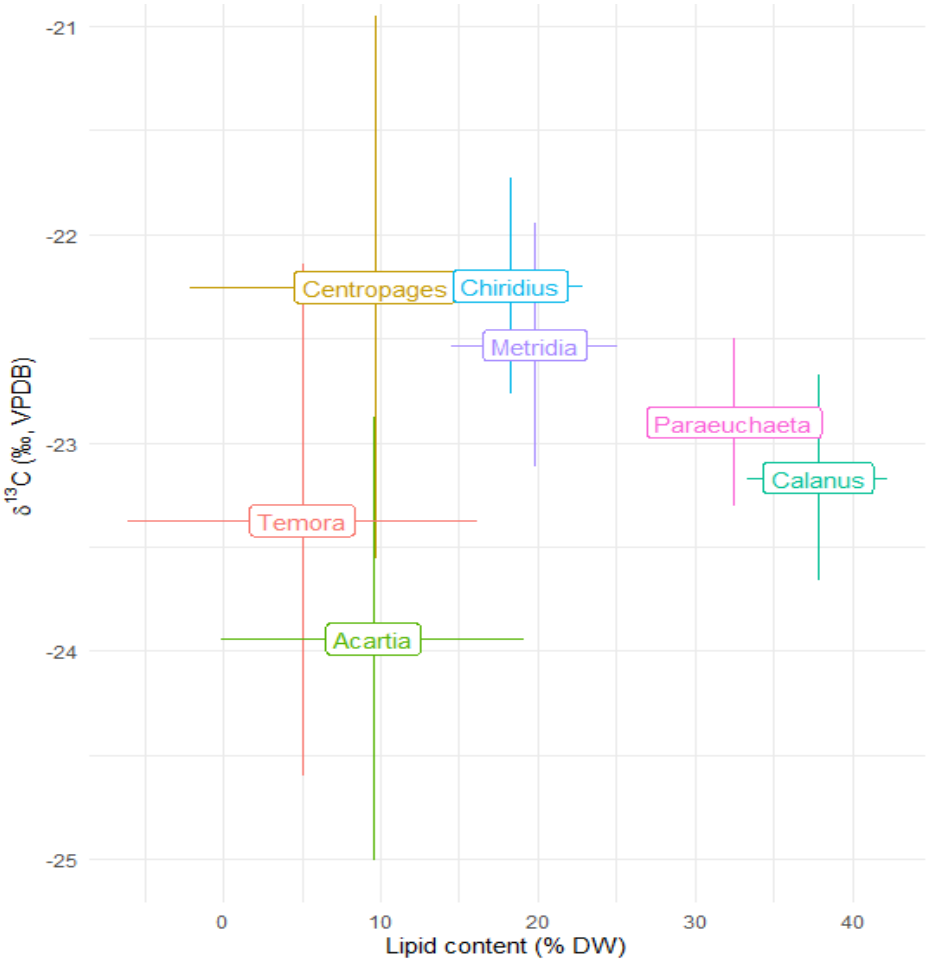

Figure 4.10: Contribution of lipids to dry weight (Lipid content (% DW)) vs $\delta^{13}C$ ratio ($\delta^{13}C$ (‰, VPDB) explained through fitted linear models from stable isotope data of 7 genera, providing mean as name tags and confidence intervals as lines. Lipid content (% DW) was estimated using equation N and C:N mass ratio from stable isotope data (Post, 2007).

5 Discussion

I found two main trophic groups with genus-specific trophic positions (Fig. 4.3). The position of these genera also vary somewhat with season, reaches a low trophic level in April and remain stable until autumn (October) (Fig. 4.9). This stability within genera is likely a consequence of genus or species traits combined with a stable environment (Kiørboe et al., 2011; Litchman et al., 2013). This pattern in trophic level for genera suggests that genus is an important unit for understanding the zooplankton food web dynamics and organism feeding, but that feeding is also affected by seasonal environmental variation (Lundsør et al., 2022; Breton et al., 2021). Furthermore, the population of each genus might affect the community as a whole, which means that life history traits such as generation time and lipid content are interesting considerations for the copepod community. In this section I will discuss what the interactions within the zooplankton food web might be and the usefulness and implications of a genusbased trophic model in the Oslofjord zooplankton community.

Where are copepods in the food web?

The stable isotope analysis of $\delta^{15}N$ and $\delta^{13}C$ infer two main zooplankton groups of trophic level 2 and 3 (Fig. 4.3, Fig. 4.4) with interactions mainly with pelagic phytoplankton and the microbial loop. Pelagic algae forms the base of the zooplankton food web, as most samples are comparable with the range of phytoplankton (-25 ‰ to -20 ‰) (Kukert & Riebesell, 1998; Meyers, 1994). However, some $\delta^{13}C$ values from *Acartia* and *Pseudocalanus* in spring (Fig. 4.4, Fig. 4.8) are comparable with a high degree of terrestrial or lake/river influence (-29 ‰ to -25 ‰) that cannot be explained by lipid fractionation (Fig. 4.8, Fig. 4.10) (Meyers, 1994; Post et al., 2007a). Overlap of $\delta^{15}N$ between copepods and POM (Storholt, 2023) (Fig. 4.2) suggest some overlap in trophic level with zooplankton, possibly due to heterotrophic protists or microzooplankton (Tiselius & Fransson, 2016). Literature on zooplankton feeding suggests that phytoplankton, protists and zooplankton are the main sources of prey (Table 5.1, references therein).

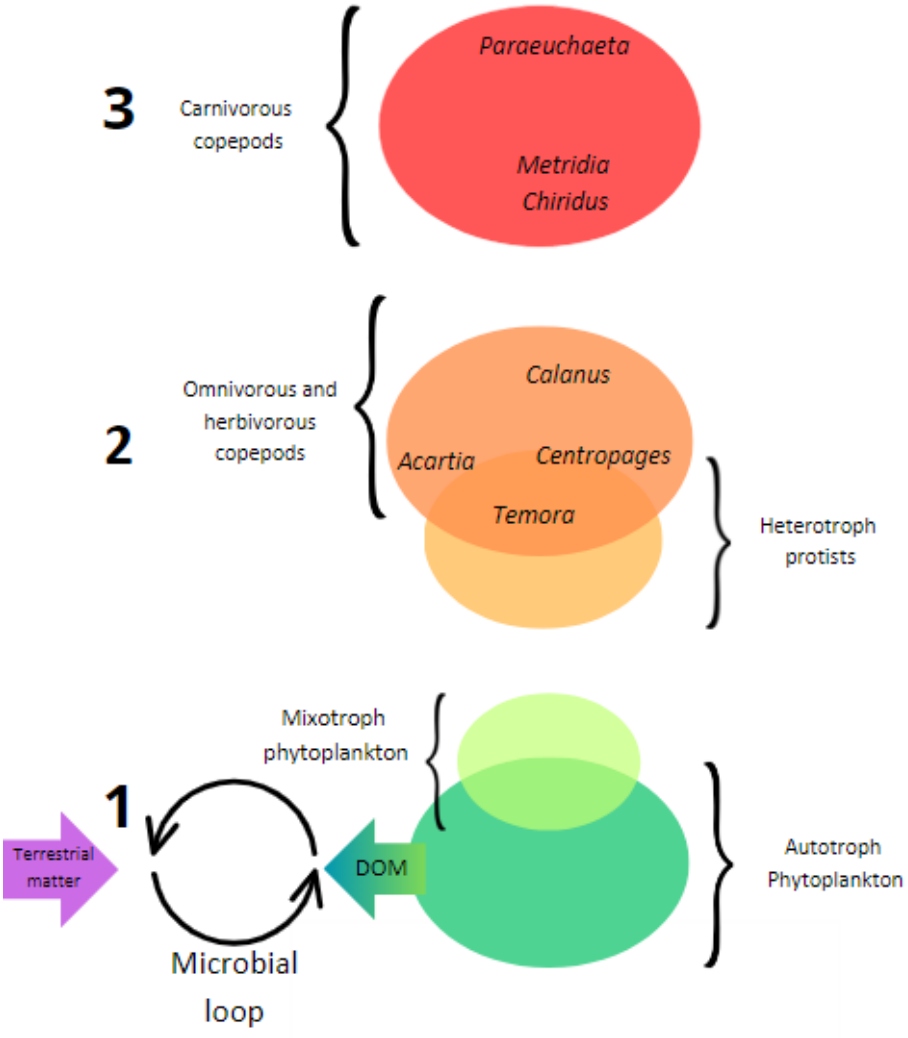

Figure 5.1: Food web sketch of the pelagic ecosystem in the Oslofjord with trophic levels 1, 2 and 3. Trophic position of the most investigated copepod genera are included in the omnivorous and carnivorous copepod groups (Fig. 4.3). The position of phytoplankton, protists and the microbial loop reflect values from POM (Fig. 4.2) and are assumed to follow other observations in the Skagerrak area (Maar et al., 2002, 2004; Nielsen & Richardson, 1989; Stoecker & Capuzzo, 1990; Tiselius & Fransson, 2016).

Table 5.1: Trait table of some important copepods and zooplankton species found in the North Sea and Oslofjord (Fransz et al., 1991). Traits (i.e., length, feeding mode) are obtained through a copepod trait database (Brun et al., 2016), while I curated prey data from other references. The three feeding modes are feeding-current feeding, ambush feeding and cruise feeding (Kiørboe, 2011). Feeding-current feeding is selective and is created by activating front limbs of copepods to create a current (van Duren et al., 2003). Ambush feeding is passive and depends on detection of motile prey. Cruise feeding is active and depends on the copepod encountering food (Kiørboe, 2011). Length data are for female adults. Trophic level is estimated from $\boldsymbol{\delta}^{15}$N of genera (Fig. 4.3) with the baseline of *Temora* and a fractionation of 3.4 ‰ $\boldsymbol{\delta}^{15}$N per trophic level. Genera with $\boldsymbol{\delta}^{15}$N below the baseline (8.7 ‰ $\boldsymbol{\delta}^{15}$N) were assigned trophic level 2.0.

*Some lengths from the database were total body lengths. These were converted to prosome length using Prosome/Body length ratios from pictures.

Genus or species name	**Prosome length (mm)**	**Feeding mode**	**Prey**	**Average trophic level of genus**	**References for prey**
Oithona similis	0.5-0.6	Ambush	Phytoplankton Protozooplankton Faecal matter	**3.3**	(Castellani et al., 2008) (González & Smetacek, 1994)
Oithona atlantica	0.6*	Ambush		**3.3**	
Calanus finmarchicus	1.9-2.4	Feeding current	Phytoplankton Protozooplankton Zooplankton	**2.5**	(Castellani et al., 2008) (Bonnet et al., 2004)
Calanus helgolandicus	2.5-3.1	Feeding current	Phytoplankton Protozooplankton Zooplankton	**2.5**	(Paffenhöfer, 1971) (Fileman et al., 2007) (Bonnet et al., 2004)
Calanus hyperboreus	5.8-8.3*	Feeding current	Phytoplankton Protozooplankton	**2.5**	(Søreide et al., 2008)
Pseudocalanus elongatus	0.8-1.1	Feeding current	Phytoplankton Protozooplankton	**2.0**	(Fileman et al., 2007)
Paracalanus parvus	0.6-0.9	Feeding current	Phytoplankton Protozooplankton	**3.3**	(Fileman et al., 2007) (Suzuki et al., 1999)
Metridia longa	2.9-3.0*	Cruise	Phytoplankton Zooplankton	**3.2**	(Vestheim et al., 2013)
Metridia lucens	1.5-1.8	Cruise	Phytoplankton Zooplankton	**3.2**	(Sell et al., 2001) (Haq, 1967)
Acartia clausi	0.9-1.2	Feeding current and ambush	Phytoplankton Protozooplankton	**2.4**	(Gismervik & Andersen, 1997) (Fileman et al., 2010)
Centropages typicus	1.6-2.0	Feeding current, ambush and cruise	Phytoplankton Protozooplankton Zooplankton	**2.2**	(Calbet et al., 2007)
Centropages hamatus	1.0 – 1.3	Feeding current, ambush and cruise	Phytoplankton Protozooplankton	**2.2**	(Saage et al., 2009)
Temora longicornis	0.9-1.1	Feeding current	Phytoplankton Protozooplankton	**2.0**	(Serandour et al., 2023)
Paraeuchaeta norvegica	6.1	Cruise	Zooplankton	**3.8**	(Fleddum et al., 2001)
Chiridius poppei	1.8-2.6	Cruise	Phytoplankton Zooplankton	**3.2**	(Schøyen & Kaartvedt, 2004) (Alvarez & Matthews, 1975)
	Class *Branchipoda*, Order *Diplostraca*				
Evadne nordmanni			Seston(Phytoplankton + Protozooplankton)	**2.0**	(Serandour et al., 2023)
Penilia			Seston (Phytoplankton + Protozooplankton)	**2.0**	(Katechakis & Stibor, 2004)

Genus seems to be the strongest predictor for trophic level compared to season because seasonal variation of δ^{15}N for genera tends to remain within either trophic groups (Fig. 4.3, Fig. 4.9). This may suggest that copepods in the Oslofjord are somewhat specialized or constrained to a trophic level based on traits shared between genera (Brito-Lolaia et al., 2022; Kiørboe, 2011; Kürten, Painting, et al., 2013). The most important traits might be feeding mode, size and vertical distribution (Kiørboe, 2011; Skarra & Kaartvedt, 2003).

There is a strong correlation between feeding mode and trophic level where cruise and ambush feeders are carnivores (i.e., *Paraeuchaeta*, *Metridia*, *Chiridius*, *Oithona*), while feeding current feeders are omnivores (i.e., *Temora*, *Centropages*, *Acartia*, *Calanus*) (Fig.4.3, Fig. 4.4). Switchers of feeding modes (i.e., *Acartia* and *Centropages*) (Brun et al., 2016; Gismervik & Andersen, 1997) are not significantly different in seasonal trophic level range compared to *Calanus* (Fig. 4.9), which suggests that the ability to switch mode is less significant for trophic position in the Oslofjord. The implication is that feeding mode contributes to the functional organization of feeding of the copepod community (Breton et al., 2021; Kenitz et al., 2017). There are several common species within each feeding mode group (Table 5.1), which should mean that there is functional redundancy. The limitations of the feeding-mode classification of the copepod community is that there is significant seasonal variation within genera of a range up to 0.9 trophic levels (Fig. 4.5). There are also differences in δ^{13}C between April samples of *Acartia* and *Pseudocalanus* and the rest of the zooplankton community, which suggests that some genera have selective feeding depending on the food availability (Serandour et al, 2023).

The trophic position of *Paracalanus* (TL = 3.3) contradicts the feeding mode pattern as it is a carnivorous feeding current feeder. It has a high trophic level compared to other samples from the same time period such as *Pseudocalanus* (April, November) (Fig. 4.4, Fig. 4.9) despite having similar detection and feeding functions to *Pseudocalanus* (Tiselius et al., 2013). Why *Paracalanus* has a high trophic level remains unclear, but differences in vertical migration behavior where it remains further down during the night than other species (*Acartia*, *Pseudocalanus*) might explain it (Gomes et al., 2004; Itoh et al., 2011; Krause & Trahms, 1982). Feeding ecology studies on *Paracalanus* show feeding on proto-zooplankton and algae relatively similar to other species (*Calanus*, *Pseudocalanus*) (Fileman et al., 2007, 2010). However, feeding experiments using food from surface (Fileman et al., 2007, 2010) or ecology studies using shallow depth intervals (0-15 meters) (Suzuki et al., 1999) could lead to

a different result than a stable isotope analysis of copepods from 0-200 meters when the copepod genera have different depth distributions. Data on depth distribution in the Oslofjord for *Paracalanus* does not exist to my knowledge, but might be an interesting point of research when combined with stable isotope data.

Size is a worse predictor for trophic level than genus and has a low effect on trophic level with an increase of approximately 0.25 TL per 10-fold increase in mass (Fig. 4.6). However, it is correlated with feeding mode, generation time and vertical distribution (Table 5.1) (Fransz et al., 1991; Schøyen & Kaartvedt, 2004; Skarra & Kaartvedt, 2003; Vestheim et al., 2013). Among the large copepods, most are cruise feeders (*Chiridius*, *Metridia*, *Paraeuchaeta*), while small copepods tend to feed using feeding currents and ambush feeding (Table 5.1).

Large copepods are more visible and are more likely to stay further down in the water column. Their depth distribution varies over the seasons with generally shallower distribution in autumn (Schøyen & Kaartvedt, 2004; Skarra & Kaartvedt, 2003; Vestheim et al., 2013). Studies on vertical migration in the Oslofjord of *Chiridius*, *Metridia* and *Paraeuchaeta* reveal a deep distribution of *Paraeuchaeta* throughout the year and a varying seasonal depth intervals for *Chiridius* and *Metridia.* These field studies show carnivorous feeding in *Paraeuchaeta* and a significant contribution of algae for *Chiridius* and *Metridia,* which contradicts the trophic level assigned from stable isotopes in my data. Kürten et al.'s stable isotope field study shows *Metridia longa* as being trophic level 2 and 3 at two different locations, which suggests that this species can vary in diet (Kürten, Painting, et al., 2013).

Succession and seasonal variation in trophic level of copepods.

The prediction of community trophic level based on SMHI's biomass data suggests a seasonal succession in the zooplankton community with higher trophic level genera in winter than summer (Fig. 4.5). This change can be explained mainly by food availability or bottom-up control (Kürten, Painting, et al., 2013). The availability of algae compared to protozooplankton is greater in the spring and summer than winter and the total production leads to vast differences in zooplankton biomass (Fig. 4.1) (Lundsør et al., 2022; Maar et al., 2002, 2004). However, higher rates of predation from jellyfish, chaetognates and possible other predators (e.g *Paraeuchaeta*, *Chiridius*, *Metridia*, *Oithona*) on feeding-current feeders may also be a factor in the succession of copepods (Breton et al., 2021; Kenitz et al., 2017).

Breton et al.'s study (2021) on seasonal ecological specialization in the phytoplankton and zooplankton community reveals that feeding mode is one of the main important factors in ecological specialization of copepods in regimes of high competition and low predation such as the spring bloom. However, regimes of high predation can reduce specialization of the plankton community in autumn as active feeders such as feeding current feeders are more prone to predation (Breton et al., 2021). By applying this perspective to my isotope data and SMHI's biomass data, one may expect a tendency towards carnivory in species that are able to switch feeding mode (*Acartia* and *Centropages*) (Gismervik & Andersen, 1997; Kiørboe et al., 2018; Saage et al., 2009) and a faster reduction in the biomass of feeding current feeders compared to passive feeders and switchers. Monthly mean δ^{15}N in the Oslofjord is stable until late autumn for *Acartia* and stable for all sampled dates (June- October) for *Centropages*. Biomass reduction at Släggö is lower for *Paracalanus* and *Centropages* compared to other genera, but there seems to be no different pattern between the ambush feeder *Oithona* and feeding current feeders of similar size (i.e., *Temora, Pseudocalanus*) (Fig. 4.1). Based on a longer seasonal prevalence of diatoms in the Oslofjord (Lundsør et al., 2022) compared to the Eastern English channel (Breton et al., 2021), it is possible that a feeding current feeding strategy is a more competetive strategy further in the season. Nevertheless, the trophic level model of Släggö do shift to a higher trophic level from summer to winter, which is highly affected by reduction of low trophic level cladocerans (*Evadne*, *Penilia*).

Biomass at Släggö is much lower in winter than summer for all genera, which is caused by reduced primary production in winter and possibly due to predation (Breton et al., 2021; Lundsør et al., 2022). The trophic level prediction is generally consistent with observations of relative trophic level of bulk zooplankton found in the North Sea, but differ in the lowest point (April vs July). Nevertheless, there is also significant spatial and interannual variation in these areas (Kürten, Frutos, et al., 2013; Kürten, Painting, et al., 2013). The true trophic level of bulk zooplankton in the Oslofjord-Skagerrak area is most likely lowest in the spring bloom (April) and with more spatial variation. there could be a different mean δ^{15}N of some key taxa (*Evadne*, *Penilia*, *Paracalanus*) if more data was available. By applying seasonal variation within genera as well, one could achieve a more accurate model (Piscia et al., 2019). Based on seasonal variation within *Calanus* and other genera (Fig. 4.9), I would expect the true value of bulk zooplankton to be lowest in April. Another important factor that the biomass model does account for is productivity. Biomass representation does not directly translate to productivity.

As many of the small species are herbivorous (Table 5.1) and fast growing (Brun et al., 2016), the trophic level of productivity can be lower than the biomass model suggests.

Evaluating the use of stable isotopes: Future interests in the Oslofjord

The food web model relies on a few assumptions. The first assumption is that the mean $\delta^{15}N$ *Temora* is trophic level 2, and serves as a baseline. *Temora* is a herbivore specialist in spring and summer (Gentsch et al., 2009; Serandour et al., 2023). Post recommends using long-lived herbivores as a baseline for trophic level such as mussels because they integrate autotrophs and seston over longer time-periods (Post, 2002). Yearly environmental reports on the Oslofjord used blue mussels with a baseline and found mean $\delta^{15}N$ between 7.5 ‰ to 8.2 ‰ (Grung et al., 2021; Ruus, 2017; Ruus et al., 2016, 2018, 2020). *Temora* has a mean $\delta^{15}N$ of 8.7 ‰, which is between 0.35 and 0.15 trophic levels above Ruus's estimates (Grung et al., 2021; Ruus, 2017; Ruus et al., 2016, 2018, 2020). The lowest $\delta^{15}N$ of taxa was the sample of *Evadne* in august, which had a $\delta^{15}N$ of approximately 6 ‰. I did not use this as a baseline because it was only one sample and because there might be seasonal differences in POM that might change estimates of baseline when integrated over short time intervals (Kürten, Painting, et al., 2013).

The second assumption is that there is an average trophic fractionation for $\delta^{15}N$ of 3.4 (SD =±1.0) ‰ and 0.4 (SD = 1.3) ‰ $\delta^{13}C$. The fractionation number 3.4 ‰ is not a natural constant but based on empirical data found for several organisms (Post, 2002). Fractionation of $\delta^{15}N$ can vary between taxa due to differences in nitrogen excretion and absorption (Caut et al., 2009; Checkley & Entzeroth, 1985). Ammonia-secreting invertebrates are expected to have a trophic fractionation of 2.08‰ compared to 2.96 ‰ for fish (Vanderklift & Ponsard, 2003). A fractionation of 2.08 ‰ with 8.7 ‰ as a baseline would increase an estimate for *Paraeuchaeta* to trophic level 4.4. Marine ecosystems in general have 4.0 trophic levels (Jake Vander Zanden & Fetzer, 2007), and a trophic fractionation of 3.4 ‰ provides estimates that fit this pattern better than Vanderklift and Ponsard's (2008) fractionation estimate. The isotopic fractionation of feeding relationships can also vary depending on specific feeding relationships. For example, the trophic fractionation between *Acartia tonsa* and their food depended on whether it was fed on a algae culture or heterotrophic protist culture by 2.4 ‰ $\delta^{15}N$ and 4.1 ‰ $\delta^{15}N$ respectively (Tiselius and Fransson, 2016). This means that there is

uncertainty in the estimates of trophic level, which is why some studies emphasize the use of additional methods (Caut et al., 2009; Gutiérrez-Rodríguez et al., 2014; Martínez del Rio et al., 2009; Perkins et al., 2014). This uncertainty is likely to entail that some estimates of trophic level from $\delta^{15}N$ could be wrong, which is why I focused on genera with a higher number of samples and monthly coverage and placed emphasis on the larger patterns such as the two trophic groups (Fig. 4.3).

Since data was only collected from one area per month, there is a problem with pseudoreplication (Hurlbert, 1984). Other stable isotope studies show similar data to mine, but there is also some spacial variation in trophic level (Kürten, Frutos, et al., 2013; Kürten, Painting, et al., 2013; Tiselius and Fransson, 2016). Therefore the data collected during this thesis might fail to apply to a wider area or several years, but can at least be used to speculate about the trophic positions in the Skagerrak area. The lower number of samples for *Evadne*, *Paracalanus* and *Pseudocalanus* used in the biomass trophic model increases the uncertainty. Future studies should acquire a larger number of samples for important genera (Fig. 4.1).

Conclusion

The copepod community in the Oslo fjord is not a homogenous group, but comprises two trophic levels of omnivorous and carnivorous copepods. I achieved my aim of finding the trophic position of important copepod genera and also found significant seasonal variation both at a community level and genera level. Feeding mode seems to be an important factor in determining the copepod community structure. Feeding current feeders (i.e., *Calanus*, *Centropages*, *Acartia*, *Temora*, *Pseudocalanus*) are generally herbivorous or omnivorous, while cruise and ambush feeders are carnivorous. Phytoplankton forms the base of the food web, but there are also signs of terrestrial coupling for some species in spring (*Pseudocalanus*, *Acartia*).

Stable isotope analysis is a great tool for providing an overview of feeding in different species and can play part in understanding community structure. Literature on feeding suggests that there are several possible prey items (i.e. different species of algae, ciliates, zooplankton) that can match with the stable isotope signatures. Future studies should have a combined approach between stable isotope analysis and more specific feeding ecology methods (i.e faecel pellet production, faecel pellet content, eDNA) in order to provide a higher resolution of the zooplankton food web. Future studies should also acquire isotope data from several stations in order to make observations accountable for more areas.This thesis shows that there is a greater potential for complexity in the zooplankton food web than commonly assumed, but that it is still possible to predict general patterns, especially when combined with a trait-based approach.

References

Alvarez, V., & Matthews, J. B. L. (1975). Experimental studies on the deep-water pelagic community of Korsfjorden, Western Norway. *Sarsia*, *58*(1), 67–78. https://doi.org/10.1080/00364827.1975.10411279

Atomic Weight of Carbon | Commission on Isotopic Abundances and Atomic Weights. (n.d.). Retrieved 8 August 2023, from https://www.ciaaw.org/carbon.htm

Bates, D., Mächler, M., Bolker, B., & Walker, S. (2015). Fitting Linear Mixed-Effects Models Using **lme4**. *Journal of Statistical Software*, *67*(1). https://doi.org/10.18637/jss.v067.i01

Baumgartner, M. F., & Tarrant, A. M. (2017). The Physiology and Ecology of Diapause in Marine Copepods. *Annual Review of Marine Science*, *9*(1), 387–411. https://doi.org/10.1146/annurev-marine-010816-060505

Bearhop, S., Adams, C. E., Waldron, S., Fuller, R. A., & Macleod, H. (2004). Determining trophic niche width: A novel approach using stable isotope analysis. *Journal of Animal Ecology*, *73*(5), 1007–1012. https://doi.org/10.1111/j.0021-8790.2004.00861.x

Bonnet, D., Titelman, J., & Harris, R. (2004). Calanus the cannibal. *Journal of Plankton Research*, *26*(8), 937–948. https://doi.org/10.1093/plankt/fbh087

Brand, W. A., Coplen, T. B., Vogl, J., Rosner, M., & Prohaska, T. (2014). Assessment of international reference materials for isotope-ratio analysis (IUPAC Technical Report). *Pure and Applied Chemistry*, *86*(3), 425–467. https://doi.org/10.1515/pac-2013-1023

Breton, E., Christaki, U., Sautour, B., Demonio, O., Skouroliakou, D.-I., Beaugrand, G., Seuront, L., Kléparski, L., Poquet, A., Nowaczyk, A., Crouvoisier, M., Ferreira, S., Pecqueur, D., Salmeron, C., Brylinski, J.-M., Lheureux, A., & Goberville, E. (2021). Seasonal Variations in the Biodiversity, Ecological Strategy, and Specialization of Diatoms and Copepods in a Coastal System With Phaeocystis Blooms: The Key Role of Trait Trade-Offs. *Frontiers in Marine Science*, *8*. https://www.frontiersin.org/articles/10.3389/fmars.2021.656300

Brito-Lolaia, M., Figueiredo, G. G. A. A. de, Neumann-Leitão, S., Yogui, G. T., & Schwamborn, R. (2022). Can the stable isotope variability in a zooplankton time series be explained by its key species? *Marine Environmental Research*, *181*, 105737. https://doi.org/10.1016/j.marenvres.2022.105737

Brun, P., Payne, M. R., & Kiørboe, T. (2016). A trait database for marine copepods [dataset]. In *Supplement to: Brun, P et al. (2017): A trait database for marine copepods. Earth System Science Data, 9(1), 99-113, https://doi.org/10.5194/essd-9-99-2017*. PANGAEA. https://doi.org/10.1594/PANGAEA.862968

Calbet, A., Carlotti, F., & Gaudy, R. (2007). The feeding ecology of the copepod Centropages typicus (Kröyer). *Progress in Oceanography*, *72*(2), 137–150. https://doi.org/10.1016/j.pocean.2007.01.003

Carlemalm, E., Villiger, W., Hobot, J. A., Acetarin, J.-D., & Kellenberger, E. (1985). Low temperature embedding with Lowicryl resins: Two new formulations and some applications. *Journal of Microscopy*, *140*(1), 55–63. https://doi.org/10.1111/j.1365-2818.1985.tb02660.x

Castellani, C., Irigoien, X., Mayor, D. J., Harris, R. P., & Wilson, D. (2008). Feeding of Calanus finmarchicus and Oithona similis on the microplankton assemblage in the Irminger Sea, North Atlantic. *Journal of Plankton Research*, *30*(10), 1095–1116. https://doi.org/10.1093/plankt/fbn074

Caut, S., Angulo, E., & Courchamp, F. (2009). Variation in discrimination factors (Δ15N and Δ13C): The effect of diet isotopic values and applications for diet reconstruction. *Journal of Applied Ecology*, *46*(2), 443–453. https://doi.org/10.1111/j.1365-2664.2009.01620.x

Cézilly, F., Thomas, F., Médoc, V., & Perrot-Minnot, M.-J. (2010). Host-manipulation by parasites with complex life cycles: Adaptive or not? *Trends in Parasitology*, *26*(6), 311–317. https://doi.org/10.1016/j.pt.2010.03.009

Checkley, D. M., Jr., & Entzeroth, L. C. (1985). Elemental and isotopic fractionation of carbon and nitrogen by marine, planktonic copepods and implications to the marine nitrogen cycle. *Journal of Plankton Research*, *7*(4), 553–568. https://doi.org/10.1093/plankt/7.4.553

DeNiro, M. J., & Epstein, S. (1977). Mechanism of Carbon Isotope Fractionation Associated with Lipid Synthesis. *Science*, *197*(4300), 261–263.
Deniro, M. J., & Epstein, S. (1981). Influence of diet on the distribution of nitrogen isotopes in animals. *Geochimica et Cosmochimica Acta*, *45*(3), 341–351. https://doi.org/10.1016/0016-7037(81)90244-1
Fileman, E., Petropavlovsky, A., & Harris, R. (2010). Grazing by the copepods Calanus helgolandicus and Acartia clausi on the protozooplankton community at station L4 in the Western English Channel. *Journal of Plankton Research*, *32*(5), 709–724. https://doi.org/10.1093/plankt/fbp142
Fileman, E., Smith, T., & Harris, R. (2007). Grazing by Calanus helgolandicus and Para-Pseudocalanus spp. On phytoplankton and protozooplankton during the spring bloom in the Celtic Sea. *Journal of Experimental Marine Biology and Ecology*, *348*(1), 70–84. https://doi.org/10.1016/j.jembe.2007.04.003
Fleddum, A., Kaartvedt, S., & Ellertsen, B. (2001). Distribution and feeding of the carnivorous copepod Paraeuchaeta norvegica in habitats of shallow prey assemblages and midnight sun. *Marine Biology*, *139*(4), 719–726. https://doi.org/10.1007/s002270100618
Forskrift om bruk av dyr i forsøk—Lovdata. (n.d.). Retrieved 19 February 2023, from https://lovdata.no/dokument/SF/forskrift/2015-06-18-761
Fransz, H. G., Colebrook, J. M., Gamble, J. C., & Krause, M. (1991). The zooplankton of the north sea. *Netherlands Journal of Sea Research*, *28*(1), 1–52. https://doi.org/10.1016/0077-7579(91)90003-J
Fredriksen, S. (2003). Food web studies in a Norwegian kelp forest based on stable isotope (δ13C and δ15N) analysis. *Marine Ecology Progress Series*, *260*, 71–81. https://doi.org/10.3354/meps260071
Gentsch, E., Kreibich, T., Hagen, W., & Niehoff, B. (2009). Dietary shifts in the copepod Temora longicornis during spring: Evidence from stable isotope signatures, fatty acid biomarkers and feeding experiments. *Journal of Plankton Research*, *31*(1), 45–60. https://doi.org/10.1093/plankt/fbn097
Gismervik, I., & Andersen, T. (1997). Prey switching by Acartia clausi:experimental evidence and implications of intraguild predation assessed by a model. *Marine Ecology Progress Series*, *157*, 247–259. https://doi.org/10.3354/meps157247
Gomes, C. L., Marazzo, A., & Valentin, J. L. (2004). The Vertical Migration Behaviour of Two Calanoid Copepods, Acartia tonsa Dana, 1849 and Paracalanus parvus (Claus, 1863) in a Stratified Tropical Bay in Brazil. *Crustaceana*, *77*(8), 941–954.
González, H. E., & Smetacek, V. (1994). The possible role of the cyclopoid copepod Oithona in retarding vertical flux of zooplankton faecal material. *Marine Ecology Progress Series*, *113*(3), 233–246.
Grung, M., Jartun, M., Bæk, K., Ruus, A., Rundberget, T., Allan, I., Beylich, B., Vogelsang, C., Schlabach, M., Hanssen, L., Borgå, K., & Helberg, M. (2021). Environmental Contaminants in an Urban Fjord, 2020. In *100*. Norsk institutt for vannforskning. https://niva.brage.unit.no/niva-xmlui/handle/11250/2838804
Gutiérrez-Rodríguez, A., Décima, M., Popp, B. N., & Landry, M. R. (2014). Isotopic invisibility of protozoan trophic steps in marine food webs. *Limnology and Oceanography*, *59*(5), 1590–1598. https://doi.org/10.4319/lo.2014.59.5.1590
Haq, S. M. (1967). Nutritional, Physiology of Metridia Lucens and M. Longa from the Gulf of Maine1. *Limnology and Oceanography*, *12*(1), 40–51. https://doi.org/10.4319/lo.1967.12.1.0040
Heath, M. r., Backhaus, J. o., Richardson, K., McKenzie, E., Slagstad, D., Beare, D., Dunn, J., Fraser, J. g., Gallego, A., Hainbucher, D., Hay, S., Jónasdóttir, S., Madden, H., Hurlbert, Stuart H. 'Pseudoreplication and the Design of Ecological Field Experiments'. Ecological Monographs 54, no. 2 (1984): 187–211. https://doi.org/10.2307/1942661.
Mardaljevic, J., & Schacht, A. (1999). Climate fluctuations and the spring invasion of the North Sea by Calanus finmarchicus. *Fisheries Oceanography*, *8*(s1), 163–176. https://doi.org/10.1046/j.1365-2419.1999.00008.x

Itoh, H., Tachibana, A., Nomura, H., Tanaka, Y., Furota, T., & Ishimaru, T. (2011). Vertical distribution of planktonic copepods in Tokyo Bay in summer. *Plankton and Benthos Research*, *6*(2), 129–134. https://doi.org/10.3800/pbr.6.129
Jake Vander Zanden, M., & Fetzer, W. W. (2007). Global patterns of aquatic food chain length. *Oikos*, *116*(8), 1378–1388. https://doi.org/10.1111/j.0030-1299.2007.16036.x
Jaspers, C. (2009). Jaspers, C. and Carstensen, J. (2009) Effect of acid Lugol solution as preservative on two representative chitineous and gelatinous zooplankton groups. Limnology and Oceanography: Methods 7: 430-435. *Limnology and Oceanography, Methods*, *7*, 430.
Johnson, J. B., & Omland, K. S. (2004). Model selection in ecology and evolution. *Trends in Ecology & Evolution*, *19*(2), 101–108. https://doi.org/10.1016/j.tree.2003.10.013
Junk, G. A., & Svec, H. J. (1958). *NITROGEN ISOTOPE ABUNDANCE MEASUREMENTS* (ISC-1138). Ames Lab., Ames, IA (United States). https://doi.org/10.2172/4145693
Katechakis, A., & Stibor, H. (2004). Feeding selectivities of the marine cladocerans Penilia avirostris, Podon intermedius and Evadne nordmanni. *Marine Biology*, *145*(3), 529–539. https://doi.org/10.1007/s00227-004-1347-1
Kenitz, K. M., Visser, A. W., Mariani, P., & Andersen, K. H. (2017). Seasonal succession in zooplankton feeding traits reveals trophic trait coupling. *Limnology and Oceanography*, *62*(3), 1184–1197. https://doi.org/10.1002/lno.10494
Kiørboe, T. (2011a). How zooplankton feed: Mechanisms, traits and trade-offs. *Biological Reviews*, *86*(2), 311–339. https://doi.org/10.1111/j.1469-185X.2010.00148.x
Kiørboe, T., Andersen, A., Langlois, V. J., Jakobsen, H. H., & Bohr, T. (2009). Mechanisms and feasibility of prey capture in ambush-feeding zooplankton. *Proceedings of the National Academy of Sciences*, *106*(30), 12394–12399. https://doi.org/10.1073/pnas.0903350106
Kiørboe, T., Møhlenberg, F., & Hamburger, K. (1985). Bioenergetics of the planktonic copepod Acartia tonsa: Relation between feeding, egg production and respiration, and composition of specific dynamic action. *Marine Ecology Progress Series*, *26*, 85–97. https://doi.org/10.3354/meps026085
Kiørboe, T., Saiz, E., Tiselius, P., & Andersen, K. H. (2018). Adaptive feeding behavior and functional responses in zooplankton. *Limnology and Oceanography*, *63*(1), 308–321. https://doi.org/10.1002/lno.10632
Kjellerup, S., & Kiørboe, T. (2012). Prey detection in a cruising copepod. *Biology Letters*, *8*(3), 438–441. https://doi.org/10.1098/rsbl.2011.1073
Krause, M., & Trahms, J. (1982). Vertical distribution of copepods (all developmental stages) and other zooplankton during spring bloom in the fladen ground area of the north sea. *Netherlands Journal of Sea Research*, *16*, 217–230. https://doi.org/10.1016/0077-7579(82)90032-1
Kukert, H., & Riebesell, U. (1998). Phytoplankton carbon isotope fractionation during a diatom spring bloom in a Norwegian fjord. *Marine Ecology Progress Series*, *173*, 127–137.
Kürten, B., Frutos, I., Struck, U., Painting, S. J., Polunin, N. V. C., & Middelburg, J. J. (2013). Trophodynamics and functional feeding groups of North Sea fauna: A combined stable isotope and fatty acid approach. *Biogeochemistry*, *113*(1), 189–212. https://doi.org/10.1007/s10533-012-9701-8
Kürten, B., Painting, S. J., Struck, U., Polunin, N. V. C., & Middelburg, J. J. (2013). Tracking seasonal changes in North Sea zooplankton trophic dynamics using stable isotopes. *Biogeochemistry*, *113*(1), 167–187. https://doi.org/10.1007/s10533-011-9630-y
Litchman, E., Ohman, M. D., & Kiørboe, T. (2013). Trait-based approaches to zooplankton communities. *Journal of Plankton Research*, *35*(3), 473–484. https://doi.org/10.1093/plankt/fbt019
Lundsør, E., Eikrem, W., Stige, L. C., Engesmo, A., Stadniczeñko, S. G., & Edvardsen, B. (2022). Changes in phytoplankton community structure over a century in relation to environmental factors. *Journal of Plankton Research*, *44*(6), 854–871. https://doi.org/10.1093/plankt/fbac055
Maar, M., Nielsen, T. G., Gooding, S., Tönnesson, K., Tiselius, P., Zervoudaki, S., Christou, E., Sell, A., & Richardson, K. (2004). Trophodynamic function of copepods, appendicularians

and protozooplankton in the late summer zooplankton community in the Skagerrak. *Marine Biology*, *144*(5), 917–933. https://doi.org/10.1007/s00227-003-1263-9
Maar, M., Nielsen, T., Richardson, K., Christaki, U., Hansen, O., Zervoudaki, S., & Christou, E. (2002). Spatial and temporal variability of food web structure during the spring bloom in the Skagerrak. *Marine Ecology Progress Series*, *239*, 11–29. https://doi.org/10.3354/meps239011
Martínez del Rio, C., Wolf, N., Carleton, S. A., & Gannes, L. Z. (2009). Isotopic ecology ten years after a call for more laboratory experiments. *Biological Reviews*, *84*(1), 91–111. https://doi.org/10.1111/j.1469-185X.2008.00064.x
Mauchline, J. (1998a). Adv. Mar. Biol. 33: The biology of calanoid copepods. *Advances in Marine Biology*. https://www.marinespecies.org/imis.php?module=ref&refid=283361
Mauchline, J. (1998b). *The biology of calanoid copepods*. Academic Press.
McConnaughey, T., & McRoy, C. P. (1979). Food-Web structure and the fractionation of Carbon isotopes in the bering sea. *Marine Biology*, *53*(3), 257–262. https://doi.org/10.1007/BF00952434
Meyers, P. A. (1994). Preservation of elemental and isotopic source identification of sedimentary organic matter. *Chemical Geology*, *114*(3–4), 289–302. https://doi.org/10.1016/0009-2541(94)90059-0
Nielsen, T. G., & Richardson, K. (1989). Food chain structure of the North Sea plankton communities: Seasonal variations of the role of the microbial loop. *Marine Ecology Progress Series*, *56*(1/2), 75–87.
Paffenhöfer, G.-A. (1971). Grazing and ingestion rates of nauplii, copepodids and adults of the marine planktonic copepod Calanus helgolandicus. *Marine Biology*, *11*(3), 286–298. https://doi.org/10.1007/BF00401275
Paffenhöfer, G.-A. (1988). Feeding Rates and Behavior of Zooplankton. *Bulletin of Marine Science*, *43*(3), 430–445.
Perkins, M. J., McDonald, R. A., van Veen, F. J. F., Kelly, S. D., Rees, G., & Bearhop, S. (2014). Application of Nitrogen and Carbon Stable Isotopes (δ15N and δ13C) to Quantify Food Chain Length and Trophic Structure. *PLoS ONE*, *9*(3), e93281. https://doi.org/10.1371/journal.pone.0093281
Peterson, B. J., & Fry, B. (1987). Stable Isotopes in Ecosystem Studies. *Annual Review of Ecology and Systematics*, *18*(1), 293–320. https://doi.org/10.1146/annurev.es.18.110187.001453
Piscia, Roberta, Michela Mazzoni, Roberta Bettinetti, Rossana Caroni, Davide Cicala, and Marina Marcella Manca. 'Stable Isotope Analysis and Persistent Organic Pollutants in Crustacean Zooplankton: The Role of Size and Seasonality'. Water 11, no. 7 (July 2019): 1490. https://doi.org/10.3390/w11071490.
POICE: The structuring role of parasite disease on zooplankton in coastal ecosystems - Department of Biosciences. (n.d.). Retrieved 19 February 2024, from https://www.mn.uio.no/ibv/english/research/sections/aqua/research-projects/poice/index.html
Post, D. M. (2002). Using Stable Isotopes to Estimate Trophic Position: Models, Methods, and Assumptions. *Ecology*, *83*(3), 703–718. https://doi.org/10.1890/0012-9658(2002)083[0703:USITET]2.0.CO;2
Post, D. M., Layman, C. A., Arrington, D. A., Takimoto, G., Quattrochi, J., & Montaña, C. G. (2007a). Getting to the fat of the matter: Models, methods and assumptions for dealing with lipids in stable isotope analyses. *Oecologia*, *152*(1), 179–189. https://doi.org/10.1007/s00442-006-0630-x
'R: The R Project for Statistical Computing'. Accessed 7 November 2023. https://www.r-project.org/.
'R-studio'. 'Download R-studio'. Accessed 7 November 2023. https://www.posit.co/.
Riegman, R., Kuipers, B. R., Noordeloos, A. A. M., & Witte, H. J. (1993). Size-differential control of phytoplankton and the structure of plankton communities. *Netherlands Journal of Sea Research*, *31*(3), 255–265. https://doi.org/10.1016/0077-7579(93)90026-O
Ruus, A. (2017). *Environmental Contaminants in an Urban Fjord, 2016*. https://niva.brage.unit.no/niva-xmlui/handle/11250/2482314

Ruus, A., Bæk, K., Petersen, K., Allan, I., Beylich, B., Schlabach, M., Warner, N. A., Borgå, K., & Helberg, M. (2018). Environmental Contaminants in an Urban Fjord, 2017. In *115*. The Norwegian Environment Agency. https://niva.brage.unit.no/niva-xmlui/handle/11250/2593147
Ruus, A., Bæk, K., Petersen, K., Allan, I., Beylich, B., Schlabach, M., Warner, N., & Helberg, M. (2016). *Environmental Contaminants in an Urban Fjord, 2015*. https://niva.brage.unit.no/niva-xmlui/handle/11250/2415340
Ruus, A., Bæk, K., Rundberget, T., Allan, I., Beylich, B., Vogelsang, C., Schlabach, M., Götsch, A., Borgå, K., & Helberg, M. (2020). *Environmental Contaminants in an Urban Fjord, 2019*. Norsk institutt for vannforskning. https://niva.brage.unit.no/niva-xmlui/handle/11250/2718861
Saage, A., Vadstein, O., & Sommer, U. (2009). Feeding behaviour of adult Centropages hamatus (Copepoda, Calanoida): Functional response and selective feeding experiments. *Journal of Sea Research*, *62*(1), 16–21. https://doi.org/10.1016/j.seares.2009.01.002
Sano, M., Makabe, R., Kurosawa, N., Moteki, M., & Odate, T. (2020). Effects of Lugol's iodine on long-term preservation of marine plankton samples for molecular and stable carbon and nitrogen isotope analyses. *Limnology and Oceanography: Methods*, *18*(11), 635–643. https://doi.org/10.1002/lom3.10390
Schøyen, M., & Kaartvedt, S. (2004). Vertical distribution and feeding of the copepod Chiridius armatus. *Marine Biology*, *145*(1), 159–165. https://doi.org/10.1007/s00227-004-1294-x
Sell, A. F., van Keuren, D., & Madin, L. P. (2001). Predation by omnivorous copepods on early developmental stages of Calanus finmarchicus and Pseudocalanus spp. *Limnology and Oceanography*, *46*(4), 953–959. https://doi.org/10.4319/lo.2001.46.4.0953
Serandour, B., Jan, K. M. G., Novotny, A., & Winder, M. (2023). Opportunistic vs selective feeding strategies of zooplankton under changing environmental conditions. *Journal of Plankton Research*, *45*(2), 389–403. https://doi.org/10.1093/plankt/fbad007
SharkWeb. (n.d.). Retrieved 13 April 2023, from https://sharkweb.smhi.se/hamta-data/
Skarra, H., & Kaartvedt, S. (2003). Vertical distribution and feeding of the carnivorous copepod Paraeuchaeta norvegica. *Marine Ecology Progress Series*, *249*, 215–222. https://doi.org/10.3354/meps249215
Søreide, J. E., Falk-Petersen, S., Hegseth, E. N., Hop, H., Carroll, M. L., Hobson, K. A., & Blachowiak-Samolyk, K. (2008). Seasonal feeding strategies of Calanus in the high-Arctic Svalbard region. *Deep Sea Research Part II: Topical Studies in Oceanography*, *55*(20), 2225–2244. https://doi.org/10.1016/j.dsr2.2008.05.024
Stibor, H., Vadstein, O., Diehl, S., Gelzleichter, A., Hansen, T., Hantzsche, F., Katechakis, A., Lippert, B., Løseth, K., Peters, C., Roederer, W., Sandow, M., Sundt-Hansen, L., & Olsen, Y. (2004). Copepods act as a switch between alternative trophic cascades in marine pelagic food webs. *Ecology Letters*, *7*(4), 321–328. https://doi.org/10.1111/j.1461-0248.2004.00580.x
Stoecker, D. K., & Capuzzo, J. M. (1990). Predation on Protozoa: Its importance to zooplankton. *Journal of Plankton Research*, *12*(5), 891–908. https://doi.org/10.1093/plankt/12.5.891
Storholt, T. A. (2023). *A tale of three methods: Estimates of primary production in the Oslofjord* [Master thesis]. https://www.duo.uio.no/handle/10852/103813
Suzuki, K., Nakamura, Y., & Hiromi, J. (1999). Feeding by the small calanoid copepod Paracalanus sp. On heterotrophic dinoflagellates and ciliates. *Aquatic Microbial Ecology*, *17*, 99–103. https://doi.org/10.3354/ame017099
The ClIPT LAB - About the Lab. (n.d.). Retrieved 19 February 2023, from http://jahrenlab.com/
The CLIPT Stable Isotope Lab—YouTube. (n.d.). Retrieved 14 November 2021, from https://www.youtube.com/playlist?list=PLu_DCJwCuJPqokrzIqTnwFBae6FztoWNa
Thomas, K., & Nielsen, T. G. (1994). Regulation of zooplankton biomass and production in a temperate, coastal ecosystem. 1. Copepods. *Limnology and Oceanography*, *39*(3), 493–507. https://doi.org/10.4319/lo.1994.39.3.0493

Tiselius, P., & Fransson, K. (2016). Daily changes in δ15N and δ13C stable isotopes in copepods: Equilibrium dynamics and variations of trophic level in the field. *Journal of Plankton Research*, *38*(3), 751–761. https://doi.org/10.1093/plankt/fbv048
Tiselius, P., Saiz, E., & Kiørboe, T. (2013). Sensory capabilities and food capture of two small copepods, Paracalanus parvus and Pseudocalanus sp. *Limnology and Oceanography*, *58*(5), 1657–1666. https://doi.org/10.4319/lo.2013.58.5.1657
Turner, J. (2004). The importance of small planktonic copepods and their roles in pelagic marine food webs. In *Zoological Studies* (Vol. 43, p. 266).
van Duren, L. A., Stamhuis, E. J., & Videler, J. J. (2003). Copepod feeding currents: Flow patterns, filtration rates and energetics. *Journal of Experimental Biology*, *206*(2), 255–267. https://doi.org/10.1242/jeb.00078
Vanderklift, M. A., & Ponsard, S. (2003). Sources of variation in consumer-diet δ15N enrichment: A meta-analysis. *Oecologia*, *136*(2), 169–182. https://doi.org/10.1007/s00442-003-1270-z
Ventura, M., & Jeppesen, E. (2009). Effects of fixation on freshwater invertebrate carbon and nitrogen isotope composition and its arithmetic correction. *Hydrobiologia*, *632*(1), 297–308. https://doi.org/10.1007/s10750-009-9852-3
Verity, P., & Smetacek. (1996). Organism life cycles, predation, and the structure of marine pelagic ecosystems. *Marine Ecology Progress Series*, *130*, 277–293. https://doi.org/10.3354/meps130277
Vestheim, H., Brucet, S., & Kaartvedt, S. (2013). Vertical distribution, feeding and vulnerability to tactile predation in *Metridia longa* (Copepoda, Calanoida). *Marine Biology Research*, *9*(10), 949–957. https://doi.org/10.1080/17451000.2013.793806
Vestheim, H., Edvardsen, B., & Kaartvedt, S. (2005). Assessing feeding of a carnivorous copepod using species-specific PCR. *Marine Biology*, *147*(2), 381–385. https://doi.org/10.1007/s00227-005-1590-0
Vestheim, H., & Kaartvedt, S. (2006). Plasticity in coloration as an antipredator strategy among zooplankton. *Limnology and Oceanography*, *51*(4), 1931–1934. https://doi.org/10.4319/lo.2006.51.4.1931
'WP2 Net Ø57/70/75 Cm, KC Denmark · Oceanography · Limnology · Hydrobiology'. Accessed 25 October 2023. https://www.kc-denmark.dk/products/plankton-nets/wp2-net-oe577075-cm.aspx.

Appendix

Appendix A: Eliassen et al.

A lipid-targeting parasite modifies appearance and energetics of a marine copepod

Lasse Krøger Eliassen[1*] Even Sletteng Garvang[1], Tom Andersen[1], Erik Engseth[1], Kåre Andre Kristiansen[2], Jannicke Wiik-Nielsen[3], Josefin Titelman[1]

1. Department of Biosciences, University of Oslo, Oslo, Norway
2. Department of Biotechnology and Food Science, Norwegian University of Science and Technology, Trondheim, Norway
3. Fish Health Research Group, Norwegian Veterinary Institute, Ås, Norway

*Correspondence: lasse.k.eliassen@ibv.uio.no

Running head: *Calanus* parasite: pigmentation and energetics

Author contributions: LKE was responsible for the experiments and data analysis and drafted the manuscript. ESG participated in the respiration experiments and contributed to data analysis. EE collected the isotope data, KAK performed the mass spectrometry and JWN performed the scanning electron microscopy. JT and TA obtained funding, supervised LKE, ESG and EE and conceptualized the study together with LKE and ESG. TA contributed to data analysis. TA and JT contributed to the writing, and all authors reviewed and provided input to drafts and approved the final version.

Abstract

Parasitism is increasingly recognized as an important driver of ecosystem processes. Copepods are fundamental trophic links in marine food webs and harbor many microeukaryotic parasites, but unreliable access to infected individuals has limited opportunities to pursue quantitative studies of parasitic costs. One exception is *Calanus* spp. infected with the Yellow-Hyphal Parasite, where infection results in pigmented hosts with a shallow vertical distribution. Divergent evolution in conventional phylogenetic markers obtained in this study prevented phylogenetic inference but confirmed that the parasite is not *Ichthyophonus hoferi* as previously thought. Here, we identified the pigments, quantified the pigment content and respiration rate and derived stable isotope signatures of infected and uninfected *Calanus* spp. to examine costs of infection. We found that the pigments were astaxanthin and β-carotene, associated with the host and parasite, respectively. Parasitized hosts had increased astaxanthin content and respiration rate and reduced lipid content. Ultrastructure imaging revealed parasitic cells attached to host lipids. Thus, the parasite has direct detrimental impacts on host energetics and fitness and indirect consequences on fitness via host ecology. We propose that the parasite produces the bright β-carotene pigment for its own physiological benefits rather than to increase host conspicuousness as could be the case if infection of *Calanus* spp. were part of a complex life cycle with multiple hosts. The trade-off between physiological benefits and conspicuousness is particularly relevant to parasite-zooplankton dynamics as zooplankton rely heavily on transparency for survival.

Introduction

The research domains of marine ecology and parasitology have largely developed independently (Lafferty, 2017; Poulin, 1995). Although fishery ecology acknowledges the importance of parasites for stocks (Kuris & Lafferty, 1992; Patterson, 1996), pelagic ecology has generally had a resource-driven focus for over a century. While much research has been devoted to quantifying the productivity and dynamics of copepods (Mauchline, 1998b), the role of parasites and other diseases on zooplankton fitness and mortality remain understudied (Hirst et al., 2010; Hirst & Kiørboe, 2002; Tang & Elliot, 2014; Verity & Smetacek, 1996). This knowledge gap contrasts the general acceptance of disease and parasites as drivers of ecological processes on many scales across terrestrial to aquatic ecosystems (Cáceres et al., 2014; P. T. J. Johnson et al., 2015).

Copepods harbor many pathogens and parasites, including viruses, bacteria, fungi, microeukaryotes, and metazoans (Bass et al., 2021). Although recognized for over a century (Chatton 1920), little is known about their microeukaryotic parasites (Bass et al., 2021). Microeukaryotic parasites can be internal (endo) or external (ecto) and typically affect host behavior, survival, and reproduction (Table 1). Some are highly virulent parasitoids that kill their host, e.g., *Syndinium* (Chatton 1920), whereas others are less virulent, *e.g.*, *Blastodinium*, but reduce fecundity (Fields et al., 2015). Others enhance predation risk by modifying behavior and appearance (Torgersen et al., 2002), and some detrimental effects are only noticeable under multiple stressors (Puckett & Carman, 2002; Xu & Burns, 1991).

While qualitative descriptions of negative parasite effects on copepods abound (Table 1), few have estimated population-level effects (i.e., Kimmerer and McKinnon 1990; Skovgaard and Saiz 2006). The reason for the small number of quantitative studies of costs probably in part

reflects the difficulty in collecting and culturing parasitized hosts (Chatton 1920; Kimmerer and McKinnon 1990; Skovgaard 2005).

Best known in marine copepods is the parasitic genus *Blastodinium*, where *B. hyalinum* reduce respiration, fecundity, feeding rate, and fecal pellet rate and size in *Calanus finmarchicus*, indicative of starvation (Fields et al., 2015). The cyclopoid *Oncaea* infected with *B. mangini* experience sterility and higher mortality (Skovgaard, 2005). Similar planktonic parasites-host systems are somewhat better understood in freshwater, especially for ciliates in copepods (Puckett & Carman, 2002; Safi et al., 2022; Weissman et al., 1993; Xu & Burns, 1991) and for *Daphnia* where model systems enable experiments.
We have relatively predictable field access to parasitized *Calanus helgolandicus*/*finmarchicus* in the Oslofjord during the autumn, allowing for quantitative studies of parasite-copepod interactions (Torgersen et al., 2002). Both *C. finmarchicus* and *C. helgolandicus* are ubiquitous in North Atlantic ecosystems (Jónasdóttir et al., 2019). In Oslofjorden, Norway *C. helgolandicus* is the prevailing species (Bagøien et al., 2000; Bucklin et al., 1999; Dale & Kaartvedt, 2000; Kaartvedt et al., 2021; Vestheim et al., 2005). As in Torgersen et al. (2002), we did not discriminate between them and henceforth refer to them as "*Calanus* spp.*"*. They typically reside deeper in the fjord during the daytime to minimize the risk of predation and feed in surface layers at nighttime (Dale & Kaartvedt, 2000). *Calanus* spp. also build up large lipid reserves to survive diapause during the autumn and winter and to fuel reproduction, which renders them ecologically important prey for planktivores (Varpe et al., 2005). Could the high lipid content also make them desirable to parasites?

The parasite in question is poorly described with only one quantitative study (Torgersen et al., 2002). It exists as yellow, "hyphal-like" clusters of cells that eventually occupy most of the copepod (Fig. 1). In contrast to healthy individuals that are mostly transparent and/or red,

parasitized *Calanus* spp. appear yellow (Fig. 1) and remain in the surface layer, even during daytime e. The yellow parasite is easily visible through the host´s carapace (Fig. 1), which typically becomes covered by deep red lines in infected hosts (Torgersen et al., 2002). The pigment in the red lines is probably astaxanthin, a common carotenoid pigment in copepods (Vilgrain et al., 2023). The yellow pigment of the parasite is identified and quantified here (this study).

Pigmentation increases detectability by visual predators (Aksnes & Utne, 1997; Gorokhova et al., 2013; Vestheim & Kaartvedt, 2006). Torgersen et al. (2002) therefore proposed that the parasite increases detection to facilitate predation by visual predators, implying that the parasite has a complex life cycle with multiple hosts (Poulin, 1995) or that the predator facilitates dispersal i.e., the "predator-spreader" hypothesis (Cáceres et al., 2009). However, the life cycle of the parasite remains unconfirmed and the host effects could be explained by alternative mechanics (Lafferty, 1999; Poulin, 1995).

The parasite was originally assigned to the fish-infecting *Ichthyophonus hoferi* (Ophistokonta, Ichthyosporea) (Chatton 1920), but this is likely incorrect (Torgersen et al., 2002), as is also suggested by our sequencing attempts (see Supporting Information Table S1). We could only assign it to Eukaryota, hence resolving the taxonomy likely requires a multi-gene phylogeny that falls outside the scope of this study. Given its uncertain taxonomy, it was referred to as the "Yellow-Hyphal Parasite" by Bass et al. (2021) and we adopt the same nomenclature here. Given the scarcity of knowledge about this parasite, and costs of parasitism in general, we aimed to describe the parasite in more detail and, as one of very few parasites that can be reliably collected, provide quantitative data related to the metabolic and ecological costs of parasite infection, including the altered pigmentation. Such data is essential for understanding potential population effects of parasite disease.

Methods

Field sampling

Sampling of *Calanus helgolandicus/finmarchicus*, took place in Drøbak, Norway in the autumns of 2020-2022, when the parasite-host system is available in the surface waters (Torgersen et al., 2002). 57 parasitized hosts (11 % C5: 89 % ♀) were collected with a WP2 plankton net (200 µm mesh size) in convergence zones or near the shore on the surface (< 20 cm depth), as in (Torgersen et al., 2002). 49 unparasitized hosts (87 % C5: 13 % ♀) were collected by vertical net hauls (0-50 m). The status as unparasitized was defined as having no visible infection as indicated by yellow color when inspected under a stereo microscope and in images. These hosts were included in the respiration experiment, imaging, and pigment analysis. Parasitized an unparasitized hosts were placed in separate containers filled with 1 µm-filtered seawater from 60 m depth, fed small amounts of Shellfish Diet 1800 (Reed Mariculture, USA) and kept at the *in-situ* surface temperature (12 °C for October 2020, and 16 °C for August 2021). The samples for stable isotope analysis (20 of each parasitized and unparasitized) were collected in November 2021. The specimens for scanning and transmission electron microscopy were collected in September 2021 and 2022, respectively.

Stable isotopes

Stable isotope signatures of parasitized and unparasitized hosts were collected to assess changes in trophic level and lipid content in the parasite-host complex. The Stable Isotope Laboratory at the University of Oslo has sufficient resolution to measure the elemental and isotopic composition of individual copepods. The analytical system consists of a Flash EA (Elemental Analyzer) with an auto-sampler linked to a Delta V Advantage IRMS (Isotope Ratio Mass Spectrometer), both from Thermo Scientific, Germany. Live copepods were briefly washed in distilled water, sorted into tin capsules, air-dried, and loaded on the auto-

sampler. The laboratory reports the isotopic composition of carbon and nitrogen ($\delta^{13}C$ and $\delta^{15}N$) as abundance ratio deviations relative to standard materials, using the same sources for reference and quality control materials as e.g., (Jourdain et al., 2020).

Size, sex, stage, lipid, and carbon content

After experiments but before pigment extractions, copepods were photographed from the lateral side, using a Canon EOS 7D camera equipped with a Canon MP-E 65mm macro lens and a SIGMA EM-140 DG macro ring flash. The copepodite stage and sex were identified. The prosome length, prosome area, and parasite area were measured using the image analysis program Fiji (V153c) (Schindelin et al., 2012). Prosome area and parasite area were measured by tracing the outline of each. We estimated the degree of infection as the percentage of parasite projection area relative to the host prosome area. Lipid content as % of dry mass (lipid %) was estimated from the C/N ratio following equation 2 of Table 1 in (Post et al., 2007b) (i.e., $Lipid\ \% = -20.54 + 7.24 \cdot C/N$). Host carbon content (C; mg) was estimated from prosome length (L; mm) following the length-dry weight regression in (Hay et al., 1991), and assuming a carbon content of 45% of dry weight (Lindley et al., 1997) (i.e., $C = 0.45 \cdot 0.0154\ L^{2.71}$). Our direct measurements of carbon in the stable isotope analysis indicated a lower carbon content than expected from the prosome length in parasitized hosts (Fig. 3a-b). The late discovery of this prevented us from directly measuring carbon content of the hosts used in the experiments. To account for the discrepancy, we applied carbon content correction factors of 0.6 and 0.9 for parasitized and unparasitized hosts, respectively.

Light, scanning, and transmission electron microscopy

Images were taken for taxonomic and anatomical descriptions of the parasite-host system. Images for measuring cell size was taken with an Axio Vert.A1 inverted microscope equipped with an Axiocam 105 color camera (both from Carl Zeiss, Germany). In preparation for scanning electron microscopy (SEM), one host and pieces of dissected parasitic tissue were

fixed with 1.25% glutaraldehyde and 2% paraformaldehyde in 0.1 M sodium cacodylate buffer (SCB) overnight. The samples were washed thoroughly in 0.1 M SCB and dehydrated through an ascending ethanol (EtOH) gradient (30 to 100% EtOH), critical point dried, mounted on steel stubs, gold/palladium ion sputtered, and analyzed on a scanning electron microscope (Hitachi S4800).

In preparation for transmission electron microscopy, the infected copepods were fixed in 4% formaldehyde and 0.8% glutaraldehyde in 1.5 x PHEM buffer (Montanaro et al., 2016; Schliwa & van Blerkom, 1981) diluted in artificial seawater. The fixation was continued for 24 h at room temperature (RT; about 25 °C) in about 1ml fixative and another 24 h at 4 °C. The samples were quenched in 100 mM glycine for 30 min at RT and embedded in a sheet of 2% low melting point agarose. For post-fixation, the sample was washed 3 times with freshly prepared 100 mM sodium bicarbonate buffer pH6.5 [HCl] and incubated for 2 h on ice with 2% osmium tetroxide and 1.5% potassium ferricyanide in 100 mM sodium bicarbonate buffer pH6.5 [HCl] (Wood & Luft, 1965). Further washing included 5 times each 5 min long with sodium bicarbonate buffer pH6.5 [HCl] and 2 times 5 min with 50 mM maleate buffer pH5.15 [NaOH] followed by 1 h incubation with 1% uranyl acetate in 50 mM maleate buffer pH5.15 [NaOH] (Reese & Karnovsky, 1967) and 2 washes of 10 min with 50 mM maleate buffer pH5.15 [NaOH]. Storage overnight was in 100mM HEPES buffer pH 7.2. A dehydration gradient was performed by PLT (Carlemalm et al., 1985) using EtOH as a solvent, starting on ice with 30% ETOH in water for 30 min and ending with 100% dry ETOH for 30 min at -25 °C, 3 times 100% dry acetone for 30 min at -25 °C and finally 25% EPON in dry acetone at RT for approximately 10 h in an open vial on a rotating wheel. EPON (Luft, 1961) was prepared in a ratio of 3:7 (DDSA:NMA) and 1% DMP-30 fresh before use. The infiltration was continued using fresh 100% EPON for 24 h on a rotating wheel, the samples were embedded in flat embedding moulds and orientated after 3 h of polymerisation at 60 °C

followed by incubation for 45 h at 60 °C and 24 h at RT (approx. 25 °C). After trimming 300µm thick sections were collected on glass coverslips and stained with 0.1% toluidine blue in 100mM borate buffer pH 11 (Mercer, 1963) for orientation in the light microscope. The samples were further sectioned at 60 nm thickness on a Leica UCT ultramicrotome using Diatome 45° ultra knives and sections were mounted on carbon coated, formvar film on 1.5 x 2 mm copper slot grids. The sections were stained with 2% uranylacetate (Huxley & Zubay, 1961) in water for 20 min and lead citrate (Reynolds, 1963) for 90 s. Imaging was performed on a Jeol JEM-1400 at 120 kV using a Tvips 216 camera.

Pigments

Pigments were identified and quantified as they entail fitness costs from enhanced detectability by predators. We made host pigment extracts by placing individual specimens in PCR tubes filled with 200 µL 96% EtOH. The tubes were placed in the dark at -20 °C for 72 h, followed by 6 h at 4 °C, then briefly vortexed and transferred to a Nunc ® 96-well Optical Bottom Plate. Blanks containing only 96 % EtOH were included.

We used the Gaussian Peak Spectra (GPS) method (Thrane et al., 2015) to both identify and quantify copepod pigments. As data input, we measured the absorption spectra from 400 to 750 nm at 1 nm increments for each extract using a Synergy™ MX Multi Detection Microplate Reader (Agilent, USA). The GPS method fits absorbance spectra of unknown pigment mixtures to weighted sums of known pigment spectra by non-negative least squares, with the known pigment spectra represented as weighted sums of Gaussian functions (Thrane et al., 2015).

After measuring the absorption spectra, the extracts from October 2020 were dried under a flow of nitrogen gas and shipped to the Norwegian University of Science and Technology (Trondheim, Norway) for analysis by liquid chromatography and mass spectrometry. The

extracts were first analyzed per animal, and then pooled into two concentrated samples, parasitized and unparasitized, to enhance the detection signal. A concentration series for astaxanthin (SML0982-50MG, Sigma-Aldrich) was included (0.1, 0.25, 0.50, 0.75, and 1.00 µM). For β-carotene (22040-1G-F, Sigma-Aldrich) only one concentration was included (10 µM). Eight extraction blanks (ethanol) and instrument blanks (acetone) were included.

Analyses were performed with an ACQUITY UPLC® system coupled to a Synapt G2Si HDMS mass spectrometer (Waters, Milford, MA, USA) equipped with an APCI source operating in positive mode. The chromatography and mass spectrometry (MS) followed the method of (Hakvåg et al., 2020), except that the corona current was set to 8.0µA, source offset to 60V, mass range to 50-2000 Da, and lock mass to 20 µL/min. Data was recorded in MSE mode with Collision Induced Disassociation (CID) energy ramped between 15 eV to 40 eV in the trap cell.

Respiration

Respiration rates were measured to quantify the metabolic impact of the infection. Respiration rates of individual copepods were measured with PreSens SDR SensorDish ® 24-channel readers (PreSens Precision Sensing, Germany) and 4 mL glass vials (SensorVial SV-PSt5-4mL), within 72 h of collection. The readers were partially submerged in water inside a temperature-controlled chamber. One copepod was added to each vial of 0.22 µm-filtered seawater and sealed airtight. Vials containing only 0.22 µm-filtered seawater were included as blanks. Experiments were conducted at 12.5 °C in October 2020 and 16.5 °C in August 2021. The experiments were ended once stable oxygen depletion curves spanning several hours were obtained.

Linear models of oxygen concentration were fitted for each vial after the removal of data from the first hour and corrected by subtracting the mean rate of the blanks. The oxygen depletion

rate (µmol O_2 L^{-1} day^{-1}) was converted to respiration rate (µg C day^{-1}) assuming a respiratory quotient of 1 (Ikeda et al., 2000) and divided by host carbon content to produce specific respiration rate (µg C µg C^{-1} day^{-1}). Respiration rates were corrected to a common temperature of 15 °C by assuming a Q_{10} of 1.95 (Ikeda et al., 2001).

Data handling

Data handling and statistics were done in R 4.2.1 (R Core Team) using Rstudio 2021.9.0.351 (Rstudio Team), with the packages tidyverse and ggplot2 (Wickham et al., 2019). Msnbase (Gatto et al., 2021) was used to access the chromatography, absorbance, and mass spectrometry raw files. Details of data analysis are included in the results, and statistics are given in the figure legends. Scripts and data are available at https://doi.org/10.5281/zenodo.10037441

Results

Parasite-host association

Yields from surface trawls varied greatly, likely due to wind and currents (see Torgersen et al. 2002). Parasitized hosts had a conspicuous, orange coloration (Fig. 1b-d). This was a combination of yellow and red pigmentation associated with the parasite and host, respectively. Infected hosts appeared vital despite the highly invasive parasite, and filtered water, ejected fecal pellets, and jumped when disturbed. Many of the parasitized hosts lived for up to two weeks *ex-situ*.

On a macroscopic scale, the parasite appeared as forked, yellow root-like structures spread throughout the host's prosome (Fig. 1). The 2d, lateral area occupied by the parasite, referred to as the degree of infection, was 67± 23% (mean ± sd, n = 60) of the host prosome. The parasite was associated with the central region of the prosome but sometimes extended into the appendages. It remains unclear whether the parasite enveloped or penetrated the lipid sac.

A thin cuticle contained the cells (Fig. 1f, g). It is not known whether this cuticle is derived from the parasite or the host. Cells contained by the cuticle were clustered into hexagonal shapes (Fig. 1g). By piercing the copepod, both intact and ruptured root-like structures could be extracted (Fig. 1). The cells that were not released upon rupturing the cuticle were connected by thin filaments (Fig. 1h). Although variable, most released cells were oval with a diameter of 6.8 ± 1.0 µm (mean ± sd, n = 29).

Transmission electron microscopy revealed that the parasite is a eukaryote with a simple nucleus and flat mitochondrial cristae (Fig. 2). The most characteristic trait of the cells was the abundance of small, lipid-rich vacuoles (LRVs) (Fig. 2b). The LRVs were often in the same area as the much larger, less contrasting vacuoles (example in Fig. 2b). Cytosis, the uptake or release of contents across the cell membrane, was observed in the hemocoel of the host (Fig. 2e). We found no morphological traits to assign the parasite to a taxonomic group.

Some cells interacted with lipid-rich host structures in the hemocoel (Fig. 2f). These cells were attached to the lipid structure. The immediate area of the lipid structure surrounding the cell was less dense than the rest of the structure. This suggests the parasite may be taking up or breaking down the lipids, thus mirroring the observations from the isotope analysis (Fig. 3).

Parasitized hosts had less body carbon than uninfected ones (infection status contrast ± standard error from a linear model = -13.8 ± 5.4 µg C / ind.; Fig. 3b). This translates to a 23 % reduction in the body mass of parasitized hosts, despite having 6.25 % longer prosomes (Fig. 3a). Parasitized individuals had lower C/N ratio (-0.31 ± 0.16 weight ratio units; Fig. 3c) and less ^{13}C depletion (+0.54 ± 0.22 ‰ VPDB; Fig. 3e) than unparasitized ones. Parasitized and unparasitized hosts had roughly the same $\delta^{15}N$ signature (+0.41 ± 0.31 ‰ AIR; Fig. 3f), and thus occupy the same trophic position.

Stored lipids in consumers are ^{13}C-depleted compared to their food source (e.g., (Post et al., 2007b). The higher C/N ratio and the more negative $\delta^{13}C$ is consistent with unparasitized hosts having higher lipid stores than parasitized ones. The lipid content estimated from the C/N ratio (Fig. 3d) by a regression model from (Post et al., 2007b) also reflects this contrast. In other words, parasitized hosts appear to be lipid-depleted compared with unparasitized hosts.

Pigments

The location and intensity of the red and yellow pigments varied between individuals (c.f. Fig. 1b, d). The pigments were identified as astaxanthin (red) and β-carotene (yellow) using chromatography, spectrophotometry and mass spectrometry (Fig. 4). The pigment content of individual copepods was quantified using the GPS method (Fig. 5). A linear model with carbon-specific pigment content as the response variable, infection status as a predictor, and the date of the experiment as a blocking factor found that parasitized hosts had 0.430 to 0.697 ng/µg more astaxanthin than unparasitized hosts (95% CI), and 0.230 to 0.405 ng/µg more β-carotene (95% CI). The latter was hence negligible or absent in most unparasitized hosts (Fig. 5).

Respiration

Although respiration rates were generally variable, parasitized hosts had a higher respiration rate (Fig. 6), as reflected in the consistent pattern between experiments. A linear model with adjusted carbon-specific respiration rate as the response variable, infection status as a predictor, and the date of the experiment as a blocking factor indicated that parasitized hosts had an increase in carbon-specific respiration rate of 0.03 ± 0.01 µg µg^{-1} day^{-1} (± SE) (Fig. 6). There were no obvious relationships between the degree of infection or pigment content and respiration rate, neither when considering pigments separately nor when combined into total pigment content.

Discussion

Copepods are favored prey to many predators (Varpe et al., 2005). In response, their biology largely revolves around minimizing predation risk through sensory capabilities, morphology, behavior and life history (Kiørboe, 2011b). For *Calanus* spp., strategies include efficient energy storage, vertical migration, body transparency, and adaptive pigmentation (Aksnes & Utne, 1997; Vestheim & Kaartvedt, 2006), which are all affected by the Yellow-Hyphal Parasite (This study; Torgersen et al. 2002). The massive presence and pigmentation of the parasite appear intimately linked to the hosts´ lipid storage, with direct costs to the host in terms of energetics (this study) and predation risk (Torgersen et al., 2002).

Life cycle, seasonal distribution and fitness of C*alanus* spp. depend on lipid dynamics (Irigoien, 2004; Jónasdóttir et al., 2015; Varpe et al., 2005). They store energy in the form of wax esters in a lipid sac (Lee et al., 2006), which may account for >50 % of dry weight (Jónasdóttir et al., 2015). Lipids provide twice the energy per unit mass compared to carbohydrates or proteins (Hadley, 1985), making them an attractive resource to parasites. The parasite was in direct contact with host-lipid structures in the hemocoel (Fig. 2), and when fully developed it was not possible to see the lipid sac (Fig. 1). While the stable isotopes indicated no change in trophic level and thus diet, they also revealed that the copepods were low in lipids compared to healthy hosts implying a heavy tax of the parasite infection on metabolic rates (Fig. 3). Depletion of lipids has many implications for the host. For example, *Calanus* spp. fuels reproduction, development, and diapause from its lipid capitals (Jónasdóttir et al., 2015; Lee et al., 2006) and will fail to enter diapause if it is too low (Baumgartner & Tarrant, 2017), resulting in high fitness costs (Irigoien, 2004).

The metabolic costs were also evident in higher specific respiration rates for infected hosts (Fig. 6). This contrasts with the reduced respiration in *C. finmarchicus* infected with

Blastodinium (Fields et al., 2015). While reduced respiration accompanies starvation in copepods (Kiørboe et al., 1985), the respiration rate may increase or decrease in response to an infection (Nhan et al., 2019). Due to the large size of the parasite in the fully developed Yellow-Hyphal Parasite-*Calanus* complex, the respiration rate reflects the metabolic activity of both the parasite and the host, hence their individual contributions cannot be resolved. However, as the copepod is the sole provider of resources to the complex, it must compensate for the net increase in metabolism by increasing foraging, altering energy allocation or conceding energy stores to the parasite, which all entail fitness costs.

The difference between infected and uninfected hosts are likely not confounded by potential host differences within the *Calanus* complex. The Yellow-Hyphal Parasite infects multiple calanoid hosts, including *C. helgolandicus*, *C. finmarchicus* and smaller coastal species (Chatton 1920). Although both *C. finmarchicus* and *C. helgolandicus* reside in Oslofjorden, *C. helgolandicus* is the dominant species (Bagøien et al., 2000; Bucklin et al., 1999; Kaartvedt et al., 2021; Vestheim et al., 2005).

Torgersen et al. (2002) proposed that the parasite has a complex life cycle based on the changes in vertical behavior and appearance. However, most changes to host phenotype do not demonstrate fitness gains for the parasite or the host (Cézilly et al., 2010; Poulin, 1995). Instead, energetic stress or harm from the infection may cause the physiological and behavioral responses (Martín-Hernández et al., 2011; Milinski, 1984). For example, in freshwater systems, the parasite *Polycaryum leave* (Chytridiomycota, Blastocladiales) has a direct life cycle where it reduces growth, castrates and increases mortality in *Daphnia* (P. T. J. Johnson et al., 2018). The infection dramatically increases the visual conspicuousness of *Daphnia* and inhibits diel vertical migration proportional to parasite load, which shows how changes similar to those observed in this study can stem from morbidity and energy depletion rather than host manipulation (P. T. J. Johnson et al., 2018). Moreover, the tendency for hosts

infected with the Yellow-Hyphal Parasite to remain near the surface may be explained by parasite-induced starvation, where it foregoes vertical migration in favor of shallow feeding; a plastic trait observed in *Calanus* spp. (Aksnes & Utne, 1997; Gorokhova et al., 2013). Visual predation risk at the surface is then further enhanced by the altered pigmentation that largely governs prey contrast (Aksnes & Utne, 1997).

The increased pigmentation comprised of astaxanthin in the host and β-carotene in the parasite (Fig. 1, 4). As a microeukaryote, the parasite probably synthesizes β-carotene from simpler molecules attained from the host (Maoka, 2020), whereas copepods depend on precursors in the diet to synthesize astaxanthin, which includes β-carotene (Sommer et al., 2006).

The distribution of astaxanthin varied greatly between individuals in our study (Fig. 1), suggesting its primary function may be unrelated to conspicuousness (c.f. Torgersen et al. 2002). Copepods with more astaxanthin appear more successful than transparent ones in terms of metabolism, reproduction, and survival (Vilgrain et al., 2023). Alternative explanations for the increase in astaxanthin include its anti-oxidative role in the immune response (Babin et al., 2019) or protection against UV radiation near the surface (Torgersen et al., 2002). Given the invasive nature of the parasite, it is possible that the β-carotene from the parasite fuels additional production of astaxanthin in the host.

Parasite-zooplankton systems differ from most other parasite-host systems in that most zooplankton rely on transparency (Perrot-Minnot et al., 2011). Any pigmentation in endoparasites, regardless of its function, can also increase host conspicuousness (Torgersen et al., 2002). As such, the β-carotene may primarily have physiological benefits related to the parasite (Vilgrain et al., 2023), rather than being a direct means to increase host conspicuousness (Torgersen et al., 2002). For example, β-carotene can protect against the

host's immune response (Babin et al., 2019; Liu et al., 2005) and the anti-oxidative property of β-carotene may protect against the UV radiation experienced near the surface (Torgersen et al., 2002), and be relevant to the rapid growth typical of microparasites (Dobson & Hudson, 1986) and survival during a potential free-living stage (Rogalski & Duffy, 2020).

The role of pigments in transparent hosts has been investigated in a comparable parasite-host system involving the transparent intermediate amphipod host *Gammarus pulex* and pigmented acanthocephalan endoparasites *Pomphorynchus* spp. (Perrot-Minnot et al., 2011). They found that pigmentation did not cause increased predation risk and pointed out that ducks, the terminal hosts of pigmented *Pomphorynchus* spp., do not rely on vision when feeding on zooplankton. The ambiguous role of carotenoids in endoparasites in transparent hosts suggests that they relate to parasite survival rather than attracting an appropriate secondary host (Cézilly et al., 2010). Indeed, *Syndinium* causes drastic changes to copepod's appearance and behavior but bursts from the host with no presumed need for a secondary host (Skovgaard et al., 2005).

In conclusion, we found that the Yellow-Hyphal Parasite affects the appearance and energetics of *Calanus* spp. with severe consequences for host fitness. Imaging revealed parasitic cells interacting with lipids, which were reduced in parasitized hosts, suggesting that the parasite targets the lipids of its host. Increased pigmentation has conventionally been linked to a complex life cycle (Poulin, 1995; Torgersen et al., 2002), but we propose that the primary function of β-carotene instead relates to its physiological benefits for the parasite (Cézilly et al., 2010; Vilgrain et al., 2023). This study highlights a pigmentation trade-off unique to endoparasites in transparent hosts that is particularly relevant to the ecology of zooplankton as they rely heavily on transparency for survival.

Acknowledgments

This is a contribution to the POICE project financed by The Research Council of Norway (RCN #315892 to JT and TA). EG was funded by a PhD fellowship from POICE, and LE by a PhD fellowship from University of Oslo and the Norwegian Ministry of Education. We thank Jens Wohlmann for ultrastructure imaging and Wenche Eikrem for discussing the images, as well as the Sindre Holm and crew of R/V Trygve Braarud, and Hans-Erik Karlsen and Grete Sørnes at the Marine Research Station Drøbak for help with collecting copepods. No conflicts of interest.

References

Aksnes, D., and A. Utne. 1997. A revised model of visual range in fish. Sarsia 82: 137–147. doi:10.1080/00364827.1997.10413647

Babin, A., J. Moreau, and Y. Moret. 2019. Storage of Carotenoids in Crustaceans as an Adaptation to Modulate Immunopathology and Optimize Immunological and Life-History Strategies. BioEssays 41: 1800254. doi:10.1002/bies.201800254

Bagøien, E., S. Kaartvedt, and S. Øverås. 2000. Seasonal vertical migrations of Calanus spp. in Oslofjorden. Sarsia 85: 299–311. doi:10.1080/00364827.2000.10414581

Bass, D., S. Rueckert, R. Stern, A. C. Cleary, J. D. Taylor, G. M. Ward, and R. Huys. 2021. Parasites, pathogens, and other symbionts of copepods. Trends Parasitol. 37: 875–889. doi:10.1016/j.pt.2021.05.006

Baumgartner, M. F., and A. M. Tarrant. 2017. The Physiology and Ecology of Diapause in Marine Copepods. Annu. Rev. Mar. Sci. 9: 387–411. doi:10.1146/annurev-marine-010816-060505

Bucklin, A., M. Guarnieri, R. S. Hill, A. M. Bentley, and S. Kaartvedt. 1999. Taxonomic and systematic assessment of planktonic copepods using mitochondrial COI sequence variation and competitive, species-specific PCR, p. 239–254. In J.P. Zehr and M.A. Voytek [eds.], Molecular Ecology of Aquatic Communities. Springer Netherlands.

Cáceres, C. E., C. J. Knight, and S. R. Hall. 2009. Predator–spreaders: Predation can enhance parasite success in a planktonic host–parasite system. Ecology 90: 2850–2858. doi:10.1890/08-2154.1

Cáceres, C. E., A. J. Tessier, M. A. Duffy, and S. R. Hall. 2014. Disease in freshwater zooplankton: what have we learned and where are we going? J. Plankton Res. 36: 326–333. doi:10.1093/plankt/fbt136

Carlemalm, E., W. Villiger, J. A. Hobot, J.-D. Acetarin, and E. Kellenberger. 1985. Low temperature embedding with Lowicryl resins: two new formulations and some applications. J. Microsc. 140: 55–63. doi:10.1111/j.1365-2818.1985.tb02660.x

Cézilly, F., F. Thomas, V. Médoc, and M.-J. Perrot-Minnot. 2010. Host-manipulation by parasites with complex life cycles: adaptive or not? Trends Parasitol. 26: 311–317. doi:10.1016/j.pt.2010.03.009

Dale, T., and S. Kaartvedt. 2000. Diel patterns in stage-specific vertical migration of Calanus finmarchicus in habitats with midnight sun. ICES J. Mar. Sci. 57: 1800–1818. doi:10.1006/jmsc.2000.0961

Dobson, A. P., and P. J. Hudson. 1986. Parasites, disease and the structure of ecological communities. Trends Ecol. Evol. 1: 11–15. doi:10.1016/0169-5347(86)90060-1

Fields, D. M., J. A. Runge, C. Thompson, S. D. Shema, R. M. Bjelland, C. M. F. Durif, A. B. Skiftesvik, and H. I. Browman. 2015. Infection of the planktonic copepod Calanus finmarchicus by the parasitic dinoflagellate, Blastodinium spp: effects on grazing, respiration, fecundity and fecal pellet production. J. Plankton Res. 37: 211–220. doi:10.1093/plankt/fbu084

Gatto, L., S. Gibb, and J. Rainer. 2021. MSnbase, Efficient and Elegant R-Based Processing and Visualization of Raw Mass Spectrometry Data. J. Proteome Res. 20: 1063–1069. doi:10.1021/acs.jproteome.0c00313

Gorokhova, E., M. Lehtiniemi, and N. H. Motwani. 2013. Trade-Offs between Predation Risk and Growth Benefits in the Copepod Eurytemora affinis with Contrasting Pigmentation. PLOS ONE 8: e71385. doi:10.1371/journal.pone.0071385

Hadley, N. F. 1985. The adaptive role of lipids in biological systems.

Hakvåg, S., I. Nærdal, T. M. B. Heggeset, K. A. Kristiansen, I. M. Aasen, and T. Brautaset. 2020. Production of Value-Added Chemicals by Bacillus methanolicus Strains Cultivated on Mannitol and Extracts of Seaweed Saccharina latissima at 50°C. Front. Microbiol. 11.

Hay, S. J., T. Kiørboe, and A. Matthews. 1991. Zooplankton biomass and production in the North Sea during the Autumn Circulation experiment, October 1987–March 1988. Cont. Shelf Res. 11: 1453–1476. doi:10.1016/0278-4343(91)90021-W

Hirst, A. G., D. Bonnet, D. V. P. Conway, and T. Kiørboe. 2010. Does predation controls adult sex ratios and longevities in marine pelagic copepods? Limnol. Oceanogr. 55: 2193–2206. doi:10.4319/lo.2010.55.5.2193

Hirst, A. G., and T. Kiørboe. 2002. Mortality of marine planktonic copepods: global rates and patterns. Mar. Ecol. Prog. Ser. 230: 195–209. doi:10.3354/meps230195

Huxley, H. E., and G. Zubay. 1961. Preferential staining of nucleic acid-containing structures for electron microscopy. J. Biophys. Biochem. Cytol. 11: 273–296. doi:10.1083/jcb.11.2.273

Ikeda, T., Y. Kanno, K. Ozaki, and A. Shinada. 2001. Metabolic rate of epipelagic copepods as a function of body mass and temperature. Mar. Biol. 139: 587–596. doi:10.1007/s002270100608

Ikeda, T., J. J. Torres, S. Hernández-León, and S. P. Geiger. 2000. 10 - Metabolism, p. 455–532. In R. Harris, P. Wiebe, J. Lenz, H.R. Skjoldal, and M. Huntley [eds.], ICES Zooplankton Methodology Manual. Academic Press.

Irigoien, X. 2004. Some ideas about the role of lipids in the life cycle of Calanus finmarchicus. J. Plankton Res. 26: 259–263. doi:10.1093/plankt/fbh030

Johnson, P. T. J., J. C. de Roode, and A. Fenton. 2015. Why infectious disease research needs community ecology. Science 349: 1259504. doi:10.1126/science.1259504

Johnson, P. T. J., D. E. Stanton, K. J. Forshay, and D. M. Calhoun. 2018. Vertically challenged: How disease suppresses Daphnia vertical migration behavior. Limnol. Oceanogr. 63: 886–896. doi:10.1002/lno.10676

Jónasdóttir, S. H., A. W. Visser, K. Richardson, and M. R. Heath. 2015. Seasonal copepod lipid pump promotes carbon sequestration in the deep North Atlantic. Proc. Natl. Acad. Sci. 112: 12122–12126. doi:10.1073/pnas.1512110112

Jónasdóttir, S. H., R. J. Wilson, A. Gislason, and M. R. Heath. 2019. Lipid content in overwintering Calanus finmarchicus across the Subpolar Eastern North Atlantic Ocean. Limnol. Oceanogr. 64: 2029–2043. doi:10.1002/lno.11167

Jourdain, E., C. Andvik, R. Karoliussen, A. Ruus, D. Vongraven, and K. Borgå. 2020. Isotopic niche differs between seal and fish-eating killer whales (Orcinus orca) in northern Norway. Ecol. Evol. 10: 4115–4127. doi:10.1002/ece3.6182

Kaartvedt, S., A. Røstad, and J. Titelman. 2021. Sleep walking copepods? Calanus diapausing in hypoxic waters adjust their vertical position during winter. J. Plankton Res. 43: 199–208. doi:10.1093/plankt/fbab004

Kimmerer, W. J., and A. D. McKinnon. 1990. High mortality in a copepod population caused by a parasitic dinoflagellate. Mar. Biol. 107: 449–452. doi:10.1007/BF01313428

Kiørboe, T. 2011. What makes pelagic copepods so successful? J. Plankton Res. 33: 677–685. doi:10.1093/plankt/fbq159

Kiørboe, T., F. Møhlenberg, and K. Hamburger. 1985. Bioenergetics of the planktonic copepod Acartia tonsa: relation between feeding, egg production and respiration, and composition of specific dynamic action. Mar. Ecol. Prog. Ser. 26: 85–97. doi:10.3354/meps026085

Kuris, A. M., and K. D. Lafferty. 1992. Modelling Crustacean Fisheries: Effects of Parasites on Management Strategies. Can. J. Fish. Aquat. Sci. 49: 327–336. doi:10.1139/f92-037

Lafferty, K. D. 1999. The evolution of trophic transmission. Parasitol. Today Pers. Ed 15: 111–115. doi:10.1016/s0169-4758(99)01397-6

Lafferty, K. D. 2017. Marine Infectious Disease Ecology. Annu. Rev. Ecol. Evol. Syst. 48: 473–496. doi:10.1146/annurev-ecolsys-121415-032147

Lee, R. F., W. Hagen, and G. Kattner. 2006. Lipid storage in marine zooplankton. Mar. Ecol. Prog. Ser. 307: 273–306. doi:10.3354/meps307273

Lindley, J. A., A. W. G. John, and D. B. Robins. 1997. Dry Weight, Carbon and Nitrogen Content of Some Calanoid Copepods from the Seas Around Southern Britain in Winter. J. Mar. Biol. Assoc. U. K. 77: 249–252. doi:10.1017/S0025315400033919

Liu, G. Y., A. Essex, J. T. Buchanan, V. Datta, H. M. Hoffman, J. F. Bastian, J. Fierer, and V. Nizet. 2005. Staphylococcus aureus golden pigment impairs neutrophil killing and promotes virulence through its antioxidant activity. J. Exp. Med. 202: 209–215. doi:10.1084/jem.20050846

Luft, J. H. 1961. Improvements in epoxy resin embedding methods. J. Biophys. Biochem. Cytol. 9: 409–414.

Maoka, T. 2020. Carotenoids as natural functional pigments. J. Nat. Med. 74: 1–16. doi:10.1007/s11418-019-01364-x

Martín-Hernández, R., C. Botías, L. Barrios, A. Martínez-Salvador, A. Meana, C. Mayack, and M. Higes. 2011. Comparison of the energetic stress associated with experimental Nosema ceranae and Nosema apis infection of honeybees (Apis mellifera). Parasitol. Res. 109: 605–612. doi:10.1007/s00436-011-2292-9

Mauchline, J. 1998. The biology of calanoid copepods, Academic Press.

Mercer, E. H. 1963. A Scheme for Section Staining in Electron Microscopy. J. R. Microsc. Soc. 81: 179–186. doi:10.1111/j.1365-2818.1963.tb02089.x

Milinski, M. 1984. Parasites determine a predator's optimal feeding strategy. Behav. Ecol. Sociobiol. 15: 35–37. doi:10.1007/BF00310212

Montanaro, J., D. Gruber, and N. Leisch. 2016. Improved ultrastructure of marine invertebrates using non-toxic buffers. PeerJ 4: e1860. doi:10.7717/peerj.1860

Nhan, J. D., C. D. Turner, S. M. Anderson, and others. 2019. Redirection of SKN-1 abates the negative metabolic outcomes of a perceived pathogen infection. Proc. Natl. Acad. Sci. 116: 22322–22330. doi:10.1073/pnas.1909666116

Patterson, K. R. 1996. Modelling the impact of disease-induced mortality in an exploited population: the outbreak of the fungal parasite (Ichthyophonus)(hoferi) in the North Sea herring (Clupea harengus). Can. J. Fish. Aquat. Sci. 53: 2870–2887. doi:10.1139/f96-234

Perrot-Minnot, M.-J., M. Gaillard, R. Dodet, and F. Cézilly. 2011. Interspecific differences in carotenoid content and sensitivity to UVB radiation in three acanthocephalan parasites exploiting a common intermediate host. Int. J. Parasitol. 41: 173–181. doi:10.1016/j.ijpara.2010.08.006

Post, D. M., C. A. Layman, D. A. Arrington, G. Takimoto, J. Quattrochi, and C. G. Montaña. 2007. Getting to the fat of the matter: models, methods and assumptions for dealing with lipids in stable isotope analyses. Oecologia 152: 179–189. doi:10.1007/s00442-006-0630-x

Poulin, R. 1995. “Adaptive” changes in the behaviour of parasitized animals: A critical review. Int. J. Parasitol. 25: 1371–1383. doi:10.1016/0020-7519(95)00100-X

Puckett, G. L., and K. R. Carman. 2002. Ciliate epibiont effects on feeding, energy reserves, and sensitivity to hydrocarbon contaminants in an estuarine harpacticoid copepod. Estuaries 25: 372–381. doi:10.1007/BF02695980

Reese, T. S., and M. J. Karnovsky. 1967. Fine structural localization of a blood-brain barrier to exogenous peroxidase. J. Cell Biol. 34: 207–217. doi:10.1083/jcb.34.1.207

Reynolds, E. S. 1963. The use of lead citrate at high pH as an electron-opaque stain in electron microscopy. J. Cell Biol. 17: 208–212. doi:10.1083/jcb.17.1.208

Rogalski, M. A., and M. A. Duffy. 2020. Local adaptation of a parasite to solar radiation impacts disease transmission potential, spore yield, and host fecundity*. Evolution 74: 1856–1864. doi:10.1111/evo.13940

Safi, L. S. L., K. W. Tang, and R. B. Carnegie. 2022. Investigating the epibiotic peritrich Zoothamnium intermedium Precht, 1935: Seasonality and distribution of its relationships with copepods in Chesapeake Bay (USA). Eur. J. Protistol. 84: 125880. doi:10.1016/j.ejop.2022.125880

Schindelin, J., I. Arganda-Carreras, E. Frise, and others. 2012. Fiji: an open-source platform for biological-image analysis. Nat. Methods 9: 676–682. doi:10.1038/nmeth.2019

Schliwa, M., and J. van Blerkom. 1981. Structural interaction of cytoskeletal components. J. Cell Biol. 90: 222–235. doi:10.1083/jcb.90.1.222

Skovgaard, A. 2005. Infection with the dinoflagellate Blastodinium in two Mediterranean copepods. Aquat. Microb. Ecol. - AQUAT MICROB ECOL 38: 93–101. doi:10.3354/ame038093

Skovgaard, A., R. Massana, V. Balagué, and E. Saiz. 2005. Phylogenetic Position of the Copepod-Infesting Parasite Syndinium turbo (Dinoflagellata, Syndinea). Protist 156: 413–423. doi:10.1016/j.protis.2005.08.002

Skovgaard, A., and E. Saiz. 2006. Seasonal occurrence and role of protistan parasites in coastal marine zooplankton. Mar. Ecol. Prog. Ser. 327: 37–49. doi:10.3354/meps327037

Sommer, F., C. Agurto, P. Henriksen, and T. Kiørboe. 2006. Astaxanthin in the calanoid copepod Calanus helgolandicus: dynamics of esterification and vertical distribution in the German Bight, North Sea. Mar. Ecol. Prog. Ser. 319: 167–173. doi:10.3354/meps319167

Tang, K., and D. T. Elliot. 2014. Copepod carcasses: Occurrence, fate and ecological importance. Copepods Divers. Habitat Behav. ISBN 978-1-63117-846-7.

Thrane, J.-E., M. Kyle, M. Striebel, S. Haande, M. Grung, T. Rohrlack, and T. Andersen. 2015. Spectrophotometric Analysis of Pigments: A Critical Assessment of a High-Throughput Method for Analysis of Algal Pigment Mixtures by Spectral Deconvolution. PLOS ONE 10: e0137645. doi:10.1371/journal.pone.0137645

Torgersen, T., E. Karlsbakk, and S. Kaartvedt. 2002. Deviating vertical distribution and increased conspicuousness of parasitized Calanus. Limnol. Oceanogr. 47: 1187–1191. doi:10.4319/lo.2002.47.4.1187

Varpe, Ø., Ø. Fiksen, and A. Slotte. 2005. Meta-ecosystems and biological energy transport from ocean to coast: the ecological importance of herring migration. Oecologia 146: 443–451. doi:10.1007/s00442-005-0219-9

Verity, P., and Smetacek. 1996. Organism life cycles, predation, and the structure of marine pelagic ecosystems. Mar. Ecol. Prog. Ser. 130: 277–293. doi:10.3354/meps130277

Vestheim, H., B. Edvardsen, and S. Kaartvedt. 2005. Assessing feeding of a carnivorous copepod using species-specific PCR. Mar. Biol. 147: 381–385. doi:10.1007/s00227-005-1590-0

Vestheim, H., and S. Kaartvedt. 2006. Plasticity in coloration as an antipredator strategy among zooplankton. Limnol. Oceanogr. 51: 1931–1934. doi:10.4319/lo.2006.51.4.1931

Vilgrain, L., F. Maps, S. Basedow, E. Trudnowska, M.-A. Madoui, B. Niehoff, and S.-D. Ayata. 2023. Copepods' true colors: astaxanthin pigmentation as an indicator of fitness. Ecosphere 14: e4489. doi:10.1002/ecs2.4489

Weissman, P., D. J. Lonsdale, and J. Yen. 1993. The effect of peritrich ciliates on the production of Acartia hudsonica in Long Island Sound. Limnol. Oceanogr. 38: 613–622. doi:10.4319/lo.1993.38.3.0613

Wickham, H., M. Averick, J. Bryan, and others. 2019. Welcome to the Tidyverse. J. Open Source Softw. 4: 1686. doi:10.21105/joss.01686

Wood, R. L., and J. H. Luft. 1965. The influence of buffer systems on fixation with osmium tetroxide. J. Ultrastruct. Res. 12: 22–45. doi:10.1016/S0022-5320(65)80004-1

Xu, Z., and C. W. Burns. 1991. Effects of the epizoic ciliate, Epistylis daphniae, on growth, reproduction and mortality of Boeckella triarticulata (Thomson) (Copepoda: Calanoida). Hydrobiologia 209: 183–189. doi:10.1007/BF00015341

Appendix B: Estimation of individual variation in d15N of *Calanus.*

Estimations of individual variation in d15N for *Calanus finmarchicus sl.* collected autumn 2021

```
library(readxl)
isotope_df = read_xlsx("C.finmarchicus_autumn.xlsx")
```

In order to find the standard deviation of dN15 in the whole dataset.

```
standard_deviation = sd(isotope_df$dN15)
summary(isotope_df$dN15)

##    Min. 1st Qu.  Median    Mean 3rd Qu.    Max.
##   7.738   8.962   9.780   9.759  10.469  12.843
```

```r
#plot(isotope_df$dN15)
x = rnorm(40, mean(isotope_df$dN15), 1)
qqplot(x, isotope_df$dN15)
```

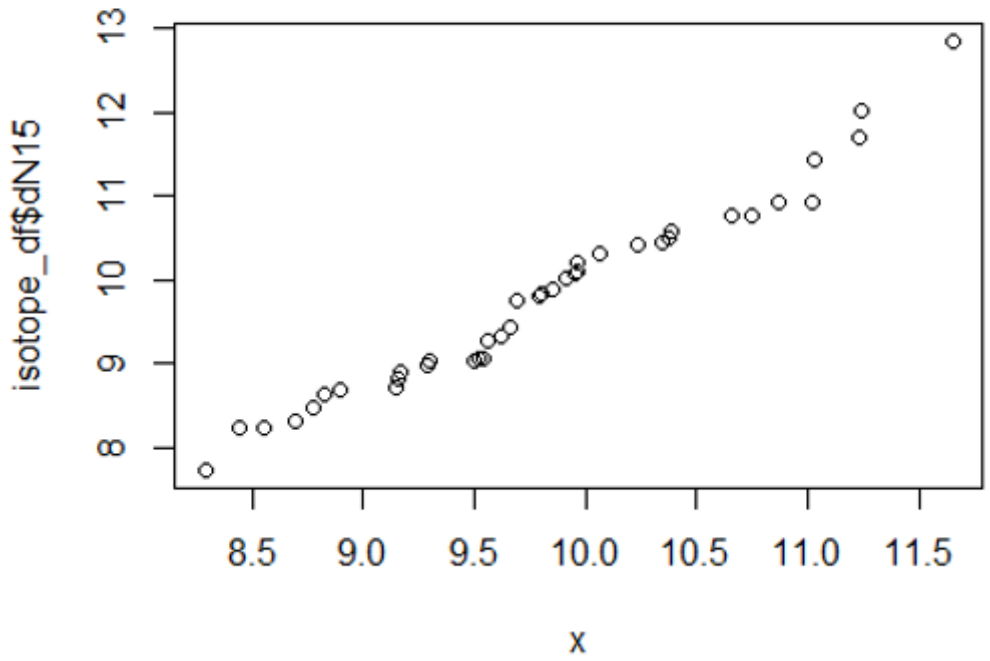

Appendix B, figure 1: quantile-quantile plot of d15N of 40 sampled individuals “isotope_df$dN15” vs constructed normal distribution “x”. Distribution of sampled individuals is similar to a normal distribution.

Expected standard error from standard deviation

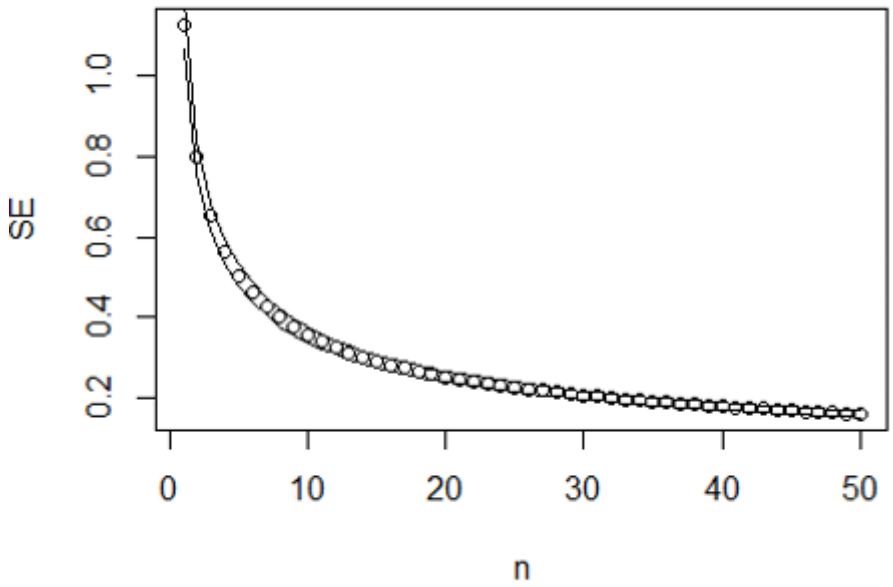

Appendix B, figure 2: Expected standard error vs sample size estimated from the standard deviation of d15N from 40 sampled individuals.

Appendix C: Hagopians appendix for stable isotope analysis.

Hagopians appendix for stable isotope analysis

Text for crediting CLIPT lab in publications/presentations/theses:

"Samples were analyzed at the CLIPT stable isotope biogeochemistry lab at UiO, funded by the Research Council of Norway through its Centers of Excellence funding scheme #223272 (Centre for Earth Evolution and Dynamics)"

Instrumentation:

For organic stable isotope analysis of bulk organic samples, we use a Thermo Fisher Scientific EA IsoLink IRMS System, which consists of a Thermo Fisher Scientific Flash Elemental Analyzer and a Thermo Fisher Scientific DeltaV Isotope Ratio Mass Spectrometer.

Analytical Sequence:

Samples containing between 0.3 and 0.7 mg carbon and 0.1 to 0.2 mg nitrogen are sealed in tin capsules, and loaded into a Costech Analytical Zero-Blank Autosampler configured with the Flash Elemental Analyzer. Within a continuous flow of helium, samples are dropped into

an oxidation reactor held at 1000 degrees Celsius. The reactor is packed with chromium oxide and silvered cobaltous/ic oxide. A pulse of oxygen is timed to arrive as the sample drops into the hottest zone of the reactor, reacting with the tin, which is an exothermic reaction that instantly elevates the combustion temperature to 1800 degrees Celsius. The chromium oxide acts as a catalyst and provides an oxidizing environment, and the silvered cobaltous/ic oxide removes any halogens and sulfur generated from the combustion. The combustion products then flow through a reduction column packed with elemental copper wires, held at 650 degrees Celsius. This removes excess oxygen not used in the combustion, and reduces NOx to N_2 gas. Water generated via combustion is removed with a chemical trap containing magnesium perchlorate. The CO_2 and N_2 are then separated via a Thermo Scientific Isolink Ramped GC Oven operated in an isothermal state at 70 degrees Celsius. The gases then flow to a Delta V stable isotope mass spectrometer for analysis. Carbon and Nitrogen elemental composition is determined from mass spectrometry peak areas.

Reference and Quality Control Materials:

Within each batch run, between 3 and 9 reps of (depending on size of run) of two internal lab reference materials (JGLUT, POPPGLY) are analyzed and used to normalize the data to the VPDB scale for $\delta^{13}C$ analysis, and the AIR scale for $\delta^{15}N$ analysis:

1) JGLUT: L-glutamic acid obtained from Fisher Scientific, $\delta^{13}C$ = -13.43‰, $\delta^{15}N$ = -4.34‰

2) POPPGLY: glycine obtained from Fisher Scientific, $\delta^{13}C$ = -36.58‰, $\delta^{15}N$ = 11.25‰

Additionally, between 3 and 9 reps (depending on size of run) of a quality control material (JALA) are incorporated into every batch run and analyzed as an unknown to assess precision and accuracy of the measurement:

JALA: alanine from Fisher Scientific, $\delta^{13}C$ = 20.62‰, $\delta^{15}N$ = -3.20‰)

All three materials (JGLUT, POPPGLY, JALA) were calibrated within our laboratory as follows:

For $\delta^{13}C$: calibrated to the VPDB scale using LSVEC (lithium carbonate, $\delta^{13}C$ = -46.6‰) and NBS- 19 (calcium carbonate, $\delta^{13}C$ = 1.95‰) (both obtained from the International Atomic Energy Agency, Vienna, Austria).

For $\delta^{15}N$: calibrated to the AIR scale using USGS40 (L-glutamic acid, $\delta^{15}N$ = -4.52‰) and USGS41 (L-glutamic acid, $\delta^{15}N$ = 47.57‰) (both obtained from the United States Geological Survey, Reston, VA, USA).

D: Additional tables, figures and Lugol recipe

Appendix D:Table 4.1: Additive model for predicting $\delta^{15}N$ from logarithmic distribution of nitrogen per animal. A linear mixed effect model describes the log-linear relationship between $\delta^{15}N$ and nitrogen per animal, which acted as a proxy for animal size. The effect of mass was fixed for all genera, while genus was a random effect, meaning they had different independent intercepts, but the same slope.

	(Intercept)	log(N.per_animal)
Calanus	9.02089	0.372354
Chiridius	11.14560	0.372354
Metridia	11.98650	0.372354
Paraeuchaeta	12.06764	0.372354

Appendix D: Table 4.2: Interactive model for prediction $\delta^{15}N$ from logarithmic distribution of nitrogen per animal. The effect of size was fixed for each genus, meaning that genus was not treated as independent or random for size-effect.

	(Intercept)	log(N.per_animal)
Calanus	8.228738	0.6550938
Chiridius	10.988919	0.4158777
Metridia	12.302616	0.2379207
Paraeuchaeta	12.530456	0.2637035

Appendix D: Table 4.3: AIC-scores for the additive linear effect model lme1 and interactive linear effect model lme2. AIC-score compares the number of independent variables and the ability of the model to reproduce data. The purpose of an AIC-score is to compare the complexity of models with how much they can explain.

	Df	AIC
lme1	4	836.1225
lme2	6	837.8506

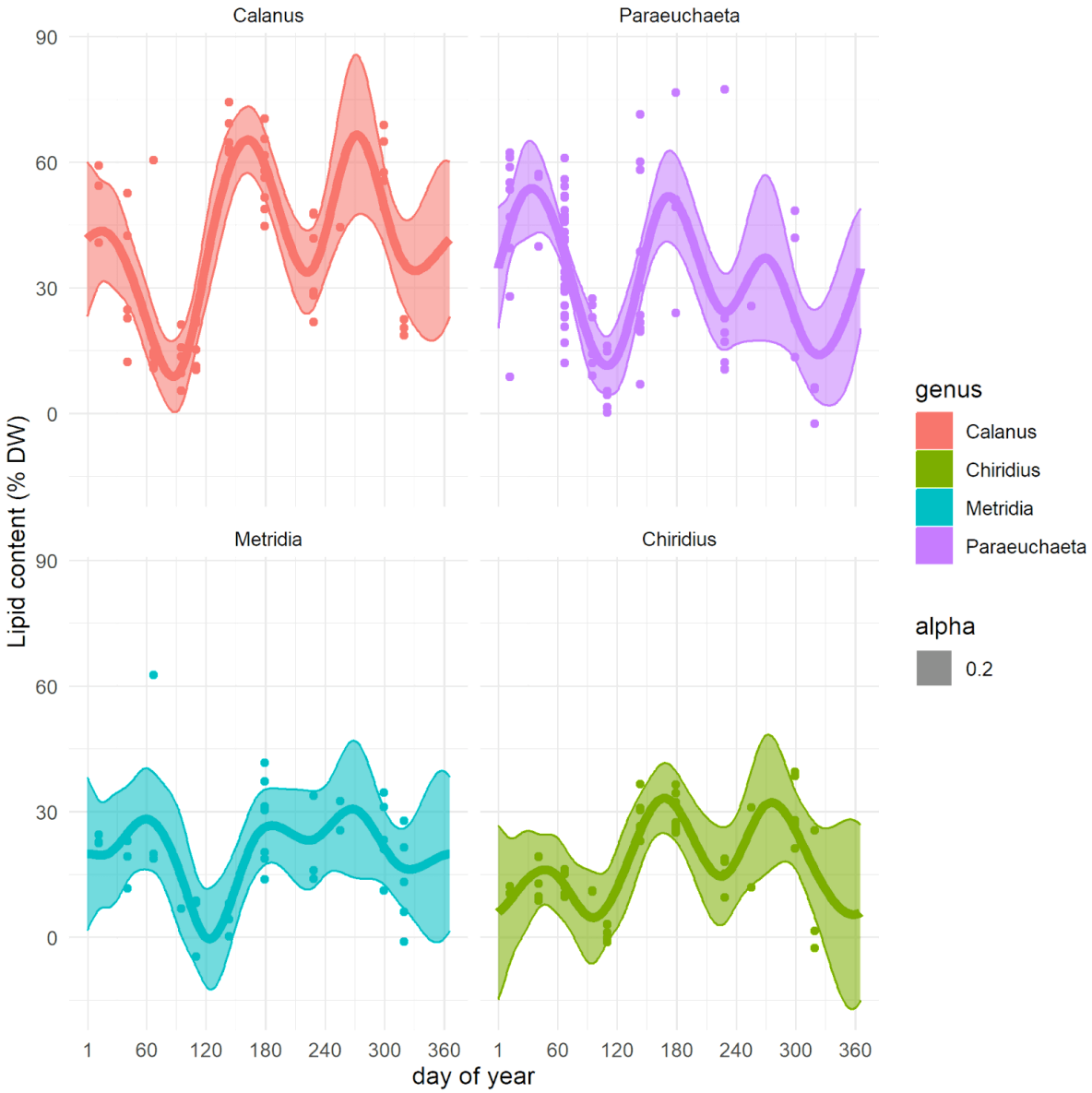

Appendix D: Figure 4.11:Time series of lipid content (%DW) for the four long-lived genera *Calanus*, *Chiridius*, *Metridia* and *Paraeuchaeta* from the IM2 station in 2022: Lipid content (%DW) was estimated using the C:N ratio and equation 4 for each stable isotope sample and compared with date of zooplankton collection and is presented as dots (Post, 2007). A generalised additive model (GAM) using a cyclic spline with factor smoothing was fitted to the data. 95 % Confidence intervals for this fit are represented by the shaded areas.

```
##
##           Acartia spp          Anomalocera sp           Appendicularia
##                    12                       2                        1
##             Brachyura            Branchiopoda Calanus finmarchicus sl
##                     3                       1                       68
##     Calanus hyperboreus          Centropages sp         Centropages spp
##                    29                       4                        5
##            Chaetognata           Chiridius sp              Cladocera
##                     3                      51                        1
```



```
##         Conchoechia spp           Euphausiacea                 Evadne
##                       1                     11                      1
##                Isopoda            Metridia sp       Oithona atlantica
##                       1                     40                      1
##         Oithona similis             Oncaea sp           Osteichthyes
##                       2                      1                      1
##         Paracalanus spp       Paraeuchaeta  sp        Paraeuchaeta sp
##                       3                      1                     84
##       Pseudocalanus sp      Pseudocalanus spp      Temora longicornis
##                       1                      3                      7
##              Temora sp               Themisto     Themisto libellula
##                       2                      1                      1
##           Tomeopteris
##                       1
```

Output from script “script_for_merging_files.Rmd”: Number of datapoints per taxa in the dataset.

Lab work:

Lab notes were taken in a physical lab journal stored at UiO.

Recipe for Lugol acetate

The recipe for Lugol used for conserving animals is the following:

25 g KI

12.5 g I^2

250 mL distilled water

25 mL acetic acid

E: Scripts, data processing and additional information

Data was handled in R. Files are available at https://drive.google.com/drive/folders/1-c_bisN3y-8kWiXiRozGEcfH7IofNN3X?usp=drive_link . The sub-folder “merging reference and isotope data” is the most organized folder and provides a curated dataset. Other folders may contain less readable or useful scripts but contribute to the figures showed in this thesis. If there are any questions regarding the files, data or how to read the files I am available at this email: erikengseth@gmail.com or erikengs@uio.no or phone-number: +47 90227805.

The folder contains scripts, raw data, overview of samples, which samples were filtered away, data processing and figures.